

Analysis of an Ultra-High Performance Concrete Two-Way Ribbed Bridge Deck Slab

August 2007

NTIS Accession No. PB2007-112112



U.S. Department of Transportation
Federal Highway Administration

FOREWORD

With the ever increasing congestion and deterioration of our nation's highway system, a need exists to develop highly durable and rapidly constructed structures. Durable bridge structures would require less intrusive maintenance and would exhibit longer life spans thus maximizing the use of the facility. Expediting bridge construction can minimize traffic flow disruptions. Ultra-high performance concrete (UHPC) is a good candidate for use in bridge decks due to its superb durability properties and enhanced mechanical properties, both of which open up possibilities for the development of new bridge systems and construction techniques.

Corrosion of mild steel reinforcement in concrete decks has long been a primary source of deck deterioration. The proposed deck design takes advantage of the high compressive strength and useable tensile capacity of UHPC to minimize the need for mild steel reinforcement. Flexural resistance of the cross section is provided by prestressing strands. This report describes the experimentally observed behavior of UHPC, a proposed design methodology, and the design/analysis of a prestressed UHPC deck element. The design example presented in this report may serve as a design aid for bridge designers and could be a vehicle in the development of design specifications for UHPC.

This report corresponds to the TechBrief titled, "Analysis of an Ultra-High Performance Concrete Two-Way Ribbed Bridge Deck Slab" (FHWA-HRT-07-055). This report only is being distributed through the National Technical Information Service for informational purposes. The content in this report is being distributed "as is" and may contain editorial or grammatical errors.

Notice

This document is disseminated under the sponsorship of the U.S. Department of Transportation in the interest of information exchange. The U.S. Government assumes no liability for the use of the information contained in this document.

The U.S. Government does not endorse products or manufacturers. Trademarks or manufacturers' names appear in this report only because they are considered essential to the objective of the document.

Quality Assurance Statement

The Federal Highway Administration (FHWA) provides high-quality information to serve Government, industry, and the public in a manner that promotes public understanding. Standards and policies are used to ensure and maximize the quality, objectivity, utility, and integrity of its information. FHWA periodically reviews quality issues and adjusts its programs and processes to ensure continuous quality improvement.

TECHNICAL REPORT DOCUMENTATION PAGE

1. Report No. FHWA-HRT-07-056	2. Government Accession No. PB2007-112112	3. Recipient's Catalog No.	
4. Title and Subtitle Analysis of an Ultra-High Performance Concrete Two-Way Ribbed Bridge Deck Slab		5. Report Date August 2007	
		6. Performing Organization Code:	
7. Author(s) Hector M. Garcia		8. Performing Organization Report No.	
9. Performing Organization Name and Address Office of Infrastructure Research and Development Federal Highway Administration 6300 Georgetown Pike McLean, VA 22101-2296		10. Work Unit No.	
		11. Contract or Grant No.	
12. Sponsoring Agency Name and Address Office of Infrastructure Research and Development Federal Highway Administration 6300 Georgetown Pike McLean, VA 22101-2296		13. Type of Report and Period Covered	
		14. Sponsoring Agency Code	
15. Supplementary Notes Additional FHWA Contacts - Benjamin A. Graybeal (Technical Advisor)			
16. Abstract Ultra-high performance concrete (UHPC) is a relatively new material which has demonstrated good durability properties, high compressive strength, and usable tensile resistance. Recent material characterization and structural behavior studies have shown the average compressive strength to be 28 ksi while a tensile strength of greater than 1.5 ksi can be maintained throughout a tensile strain of approximately 0.010. These desirable mechanical properties make UHPC a worthy material for use in our nation's highly stressed bridge decks. Since UHPC exhibits a unique flexural behavior, a design methodology must be developed to distinguish it from traditional reinforced concrete behavior. This report details UHPC flexural behavior, presents a design methodology, and presents the analysis of a two-way ribbed precast bridge deck. With the absence of design specifications for UHPC, the 2006 AASHTO LRFD Bridge Design Specifications were used where appropriate in the design and analysis of the bridge deck. From the proposed design methodology, mechanics of materials, and strain compatibility, the UHPC deck cross section in this report is analyzed for positive and negative moment capacities. The analysis reveals the proposed UHPC deck design to be capable of resisting the developed design loads. Further verification through physical testing of a full-scale UHPC two-way ribbed deck slab is recommended.			
17. Key Words Ultra-high performance concrete, UHPC, fiber-reinforced concrete, bridges, bridge deck, precast concrete, prestressed concrete, bridge design		18. Distribution Statement No restrictions. This document is available through the National Technical Information Service, Springfield, VA 22161.	
19. Security Classif. (of this report) Unclassified	20. Security Classif. (of this page) Unclassified	21. No. of Pages 64	22. Price Code A05

SI* (MODERN METRIC) CONVERSION FACTORS

APPROXIMATE CONVERSIONS TO SI UNITS

Symbol	When You Know	Multiply By	To Find	Symbol
LENGTH				
in	inches	25.4	millimeters	mm
ft	feet	0.305	meters	m
yd	yards	0.914	meters	m
mi	miles	1.61	kilometers	km
AREA				
in ²	square inches	645.2	square millimeters	mm ²
ft ²	square feet	0.093	square meters	m ²
yd ²	square yard	0.836	square meters	m ²
ac	acres	0.405	hectares	ha
mi ²	square miles	2.59	square kilometers	km ²
VOLUME				
fl oz	fluid ounces	29.57	milliliters	mL
gal	gallons	3.785	liters	L
ft ³	cubic feet	0.028	cubic meters	m ³
yd ³	cubic yards	0.765	cubic meters	m ³
NOTE: volumes greater than 1000 L shall be shown in m ³				
MASS				
oz	ounces	28.35	grams	g
lb	pounds	0.454	kilograms	kg
T	short tons (2000 lb)	0.907	megagrams (or "metric ton")	Mg (or "t")
TEMPERATURE (exact degrees)				
°F	Fahrenheit	5 (F-32)/9 or (F-32)/1.8	Celsius	°C
ILLUMINATION				
fc	foot-candles	10.76	lux	lx
fl	foot-Lamberts	3.426	candela/m ²	cd/m ²
FORCE and PRESSURE or STRESS				
lbf	poundforce	4.45	newtons	N
lbf/in ²	poundforce per square inch	6.89	kilopascals	kPa

APPROXIMATE CONVERSIONS FROM SI UNITS

Symbol	When You Know	Multiply By	To Find	Symbol
LENGTH				
mm	millimeters	0.039	inches	in
m	meters	3.28	feet	ft
m	meters	1.09	yards	yd
km	kilometers	0.621	miles	mi
AREA				
mm ²	square millimeters	0.0016	square inches	in ²
m ²	square meters	10.764	square feet	ft ²
m ²	square meters	1.195	square yards	yd ²
ha	hectares	2.47	acres	ac
km ²	square kilometers	0.386	square miles	mi ²
VOLUME				
mL	milliliters	0.034	fluid ounces	fl oz
L	liters	0.264	gallons	gal
m ³	cubic meters	35.314	cubic feet	ft ³
m ³	cubic meters	1.307	cubic yards	yd ³
MASS				
g	grams	0.035	ounces	oz
kg	kilograms	2.202	pounds	lb
Mg (or "t")	megagrams (or "metric ton")	1.103	short tons (2000 lb)	T
TEMPERATURE (exact degrees)				
°C	Celsius	1.8C+32	Fahrenheit	°F
ILLUMINATION				
lx	lux	0.0929	foot-candles	fc
cd/m ²	candela/m ²	0.2919	foot-Lamberts	fl
FORCE and PRESSURE or STRESS				
N	newtons	0.225	poundforce	lbf
kPa	kilopascals	0.145	poundforce per square inch	lbf/in ²

*SI is the symbol for the International System of Units. Appropriate rounding should be made to comply with Section 4 of ASTM E380.
(Revised March 2003)

TABLE OF CONTENTS

CHAPTER 1. INTRODUCTION.....	1
1.1 OBJECTIVE	1
1.2 TRADITIONAL REINFORCED CONCRETE DECKS	1
1.2.1 Modjeski and Masters, Inc. Bridge Deck Design	3
1.2.2 Michael Baker, Inc. Bridge Deck Design	4
1.3 REPORT OUTLINE.....	5
CHAPTER 2. UHPC FLUXURAL STRENGTH ANALYSIS METHODOLOGY.....	7
2.1 PRESTRESSED CONCRETE FLEXURAL BEHAVIOR.....	7
2.2 PRESTRESSED UHPC FLEXURAL BEHAVIOR	9
CHAPTER 3. UHPC DECK SLAB DESIGN LOADS	15
3.1 DECK SLAB PARAMETERS	15
3.1.1 T-Beam Cross Section	16
3.1.2 Material Properties.....	17
3.1.3 Concrete Parapet Properties.....	17
3.2 METHOD OF DETERMINING DESIGN LOADS	17
3.3 INTERIOR DECK DESIGN LOADS.....	18
3.3.1 Positive Moment.....	19
3.3.2 Negative Moment.....	19
3.4 OVERHANG DESIGN LOADS	20
3.4.1 Design Case I: Transverse and Longitudinal Collision Forces.....	20
3.4.2 Design Case II: Vertical Collision Force.....	30
3.4.3 Design Case III: Dead and Live Loads.....	30
3.5 SUMMARY OF DESIGN LOADS.....	36
CHAPTER 4. FLEXURAL CAPACITY ANALYSIS OF UHPC DECK SLAB.....	37
4.1 PARAMETERS AND ASSUMPTIONS.....	38
4.2 POSITIVE BENDING MOMENT CAPACITY	39
4.3 NEGATIVE BENDING MOMENT CAPACITY.....	45
CHAPTER 5. OVERVIEW OF DESIGN LOADS AND MOMENT CAPACITY.....	53
REFERENCES.....	55

LIST OF FIGURES

Figure 1. Illustration. Modjeski and Masters, Inc. Design Cross Sections.....	4
Figure 2. Illustration. Michael Baker, Inc. Design Cross Sections.....	5
Figure 3. Illustration. Prestressed Concrete Internal Stress Behavior	7
Figure 4. Graph. Experimental and Simplified UHPC Uniaxial Stress-Strain Behavior	10
Figure 5. Illustration. Prestressed UHPC Internal Stress Behavior	11
Figure 6. Illustration. Flowchart for Determining Moment Capacity for UHPC Beams	13
Figure 7. Illustration. UHPC Bridge Deck Panel Plan and Cross Section View	15
Figure 8. Illustration. UHPC Transverse Strip Cross Section	16
Figure 9. Illustration. Sections for the Overhang Region	20
Figure 10. Illustration. Section A-A of the Overhang	21
Figure 11. Illustration. Section B-B of the Overhang.....	23
Figure 12. Illustration. Distribution of Collision Moment.....	24
Figure 13. Illustration. Section C-C of the Overhang.....	26
Figure 14. Illustration. Approximate Moment Diagram between Exterior Girder and First Interior Girder Due to Dead Loads on Overhang.	27
Figure 15. Illustration. Approximate Moment Diagram between Exterior Girder and First Interior Girder Due to Dead Loads on Interior Spans.....	28
Figure 16. Illustration. Approximate Moment Diagram between Exterior Girder and First Interior Girder Due to Collision Capacity Moment.....	29
Figure 17. Illustration. Section D-D of the Overhang	31
Figure 18. Illustration. Section E-E of the Overhang	33
Figure 19. Illustration. Free Body Diagram for Section E-E.....	34
Figure 20. Illustration. UHPC Transverse Strip Cross Section	37
Figure 21. Graph. Prestressing Strand Stress Strain Model.....	38
Figure 22. Illustration. Strand Location and Force on Cross Section.....	40
Figure 23. Illustration. Cross Section Strain before Positive Bending	41
Figure 24. Illustration. Strain at Moment Capacity for Positive Bending	42
Figure 25. Illustration. Cross Section Stress Distribution for Positive Bending	43
Figure 26. Illustration. Cross Section Forces for Positive Bending.....	44
Figure 27. Illustration. Cross Section Strain before Negative Bending.....	45
Figure 28. Illustration. Strain at Moment Capacity for Negative Bending.....	47
Figure 29. Illustration. Cross Section Stress Distribution for Negative Bending.....	48

Figure 30. Illustration. Cross Section Forces for Negative Bending	49
Figure 31. Illustration. Strain Superposition for Interaction Curve	50
Figure 32. Graph. Interaction Curve for Negative Bending and Axial Tension.....	51

LIST OF TABLES

Table 1. Examples of Traditional Bridge Superstructure Properties	2
Table 2. Examples of Traditional Bridge Design Loads.....	3
Table 3. Nominal Moment Capacity of Modjeski and Masters, Inc. Deck Design.....	4
Table 4. Nominal Moment Capacity of Michael Baker, Inc. Deck Design.....	5
Table 5. T-Beam Dimensions	16
Table 6. Material Properties and UHPC Limiting Parameters	17
Table 7. Type-F Concrete Parapet Properties	17
Table 8. Load Combinations and Load Factor.....	18
Table 9. Section B-B and D-D Negative Dead Load Moments.....	32
Table 10. Section C-C and E-E Negative Dead Load Moments.....	35
Table 11. Design Moments for Interior Deck Region	36
Table 12. Design Negative Moments for Overhang Region.....	36
Table 13. T-Beam Dimensions	37
Table 14. T-Beam Properties	37
Table 15. Deck Panel Material Properties.....	38
Table 16. Design Moments/Forces and Moment Capacities	53

CHAPTER 1. INTRODUCTION

Ultra-high performance concrete (UHPC) is in a relatively new class of cementitious materials. These concretes demonstrate good durability properties, high compressive strength, and usable tensile resistance.^(1,2) The high compressive and useable tensile resistance can lead to smaller and more efficient precast cross sections. Smaller precast cross sections result in lower member self-weights, which in turn can allow for easier transportation, longer span or shallower depth superstructures, and reduced foundation requirements. The durability properties of UHPC specifically lend themselves toward use in the most environmentally stressed portions of our nation's bridge inventory, namely the decks.

The advanced properties of UHPC allow for the development of new structural systems. This report focuses on the development of a precast full-depth bridge deck component that can be used both in new construction as well as in the redecking of existing bridges. A two-way ribbed slab system shows promise when combined with the properties of UHPC.⁽³⁾ As compared to standard cast-in-place concrete bridge decks, this system can be lighter in weight, develop composite action from built-in pockets, utilize the durability properties of UHPC while decreasing the volume of required material, and efficiently use the UHPC tensile and compressive resistances.

The intent of this report is to present the transverse flexural analysis of a UHPC two-way ribbed precast, prestressed bridge deck element. Currently a set of design specifications for UHPC in the United States is not available. The 2006 AASHTO LRFD Bridge Design Specifications served as guidance in establishing design loads for the UHPC deck system. Flexural capacity for the UHPC element was determined by applying the principles of mechanics, strain compatibility, and findings from the associated material characterization and structural behavior studies.^(1, 2)

1.1 OBJECTIVE

The objective of this report is to present the transverse flexural analysis of a UHPC two-way ribbed precast, prestressed bridge deck element.

1.2 TRADITIONAL REINFORCED CONCRETE DECKS

As previously mentioned, the advanced material properties of UHPC allow for the development of new structural systems. The following illustrates the potential weight savings that can result from the use of UHPC two-way ribbed precast deck elements if used in place of a standard cast-in-place concrete bridge deck. A 2-foot wide strip of a typical cast-in-place concrete bridge deck is 7 to 8.5 inches thick and has a self-weight of about 175 to 215 pounds per linear foot. A 2-foot wide strip of the UHPC cross section developed in this report is 110 pounds per linear foot. This amounts to a 37 to 49% reduction in self-weight. The lower self-weight helps reduce the flexural demand in the deck and in the girders, helps reduce the load on the foundation, and allows for easier transportation and handling of the precast components.

To demonstrate how the UHPC deck in this report compares to tradition reinforced concrete decks, two deck designs are presented and discussed in this section. The two deck designs are taken from publications by Modjeski and Masters, Inc.⁽⁴⁾ and Michael Baker, Inc.⁽⁵⁾. The bridge superstructure geometry and parapet information for each design is listed in Table 1. The primary difference between these decks is that the Modjeski and Masters, Inc. deck is designed to be placed on prestressed concrete girders while the Michael Baker, Inc. deck is designed for steel plate girders. Both of the decks in Table 1 used a concrete with a 28-day compressive strength of 4.0 ksi and reinforcing steel with yield strength of 60 ksi.

Table 1. Examples of Traditional Bridge Superstructure Properties

Parameter	Modjeski and Masters, Inc.	Michael Baker, Inc.
Superstructure type	Reinforced concrete deck on simple span prestressed concrete girder	Reinforced concrete deck on simple span steel plate girder
Span	Two spans at 110 ft. each	Two spans at 120 ft. each
Deck width	55' 4 ½" edge to edge distance	46' 10 ½" edge to edge distance
Number of girders	6	5
Girder spacing	9' 8"	9' 9"
Overhang length	3' 6 ¼" from center line of exterior girder to overhang edge	3' 11 ¼" from center line of exterior girder to overhang edge
Parapet collision moment capacity	17.83 kip-ft/ft	28.21 kip-ft/ft
Parapet transverse resistance	137.22 kip	117.40 kip
Parapet self-weight	650 lb/ft	530 lb/ft

Design load analyses for both example decks were performed according to the 1998 AASHTO LRFD Bridge Design Specifications. Each deck is analyzed for three behavior mechanisms which are positive bending between interior girders, negative bending over interior girders, and negative bending in the overhang. Negative bending in the overhang is accompanied by an axial force resulting from an impact on the bridge railing when analyzing the Extreme Event II limit state. Example design load values for the three different regions of a 2-foot wide reinforced deck section are tabulated in Table 2. Values are given for a 2-foot section width to allow for direct comparison to the UHPC cross section analyzed in this report, as it has a spacing of 2 feet between rib elements.

Table 2. Examples of Traditional Bridge Design Loads

Region	Modjeski and Masters, Inc.	Michael Baker, Inc.
Positive bending between interior girders	26.76 k-ft	24.42 k-ft
Negative bending over interior girders	17.90 k-ft	27.44 k-ft
Negative bending and axial force in overhang at face of parapet	37.92 k-ft 10.02 kip	57.94 k-ft 11.84 kip

As seen in Table 2, the positive design moments are similar for both decks since girder spacing was nearly identical. However, negative bending over interior girders and in the overhang differed between the concrete girder and steel plate girder superstructure. The difference associated with the negative design moment over interior girders is attributed to the instruction given in AASHTO LRFD Bridge Design Specifications for the location of the design section for negative moment. Design sections for negative moment measured from the centerline of the exterior girder for the concrete and steel plate girders are 14 and 3 inches, respectively for these examples. A smaller distance to the negative design section coupled with a slightly deeper cast-in-place concrete deck results in a larger negative design moment to develop over interior girders for the steel plate superstructure. Negative bending in the overhang is greatly influenced by the collision capacity of the parapet used in the system. As seen in Table 1, there is over a 10 kip-ft difference in collision capacity between the two parapets. A combination of the collision moment capacity of the parapet and overhang self-weights contribute to a higher overhang negative moment for the steel plate superstructure design.

Reinforced concrete cross sections as designed by Modjeski and Masters, Inc. and Michael Baker, Inc. are given in the following sections. Both examples have particular designs for the different regions of the bridge deck. The nominal transverse moment capacities for the different cross sections are provided for both the cross section width and a cross section width of 2 feet as listed in Tables 3 and 4.

1.2.1 Modjeski and Masters, Inc. Bridge Deck Design

The Modjeski and Master, Inc. reinforced deck slab design is 8 inches thick along the interior regions of the deck and 9 inches thick in the overhang region. The top ½ inch is treated as an integral wearing surface and assumed not to contribute to the cross section resistance. For positive bending between interior girders, the reinforcement provided is #5 bars evenly spaced at 7 inches with a bottom cover of 1 inch as shown in Figure 1a. For negative bending over interior girders, #5 bars are spaced at 8 inches with a top cover of 2 ½ inches as illustrated in Figure 1b. The overhang design consists of #5 and #4 bars bundled together and evenly spaced at 8 inches with a top cover of 2 ½ inches as shown in Figure 1c.

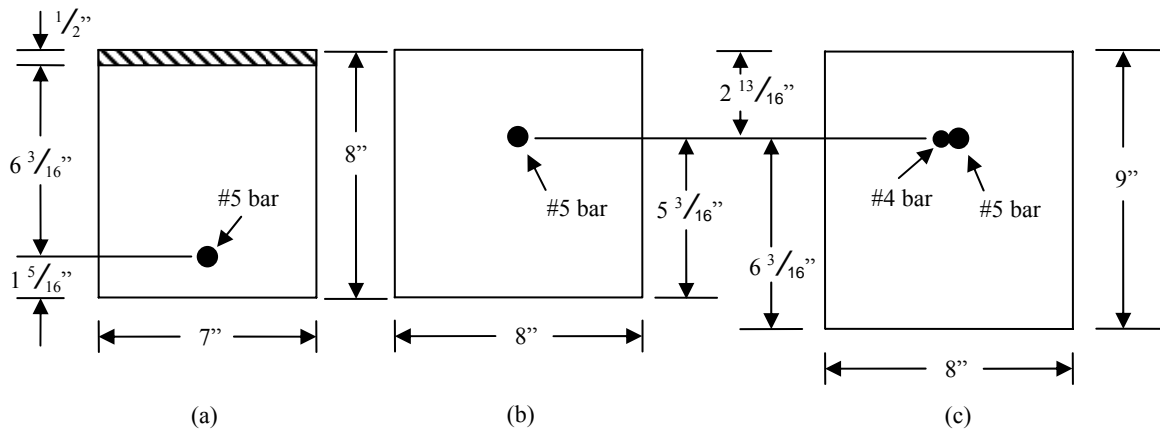


Figure 1. Illustration. Modjeski and Masters, Inc. Design Cross Sections

As a result of the impracticality of providing exact area and spacing of reinforcement steel, designers typically produce a conservative design by providing more steel than required and reducing spacing of the reinforcement steel to a more constructible pattern. Thus, the nominal moment capacity of a cross section could be significantly greater than the design moment. Table 3 provides the nominal transverse moment capacity (before applying a resistance factor) for the deck supported on prestressed concrete girders.

Table 3. Nominal Moment Capacity of Modjeski and Masters, Inc. Deck Design

Region	Per cross section width	Per 2 foot width
Positive bending between interior girders	8.98 k-ft per 7 inches	30.79 k-ft
Negative bending over interior girders	7.51 k-ft per 8 inches	22.53 k-ft
Negative bending in overhang	14.34 k-ft per 8 inches	43.02 k-ft

1.2.2 Michael Baker, Inc. Bridge Deck Design

The Michael Baker, Inc. reinforced deck slab design is 8 ½ inches thick over the interior regions of the deck and 9 inches thick in the overhang region. The top ½ inch is treated as an integral wearing surface and assumed not to contribute to the cross section resistance. For positive bending between interior girders, the reinforcement provided is #5 bars evenly spaced at 8 inches with a bottom cover of 1 inch as shown in Figure 2a. For negative bending over interior girders, #5 bars are spaced at 6 inches with a top cover of 2 ½ inches as illustrated in Figure 2b. The overhang design consists of two #5 bars bundled together and evenly spaced at 6 inches with a 2 ½ inch top cover as shown in Figure 2c.

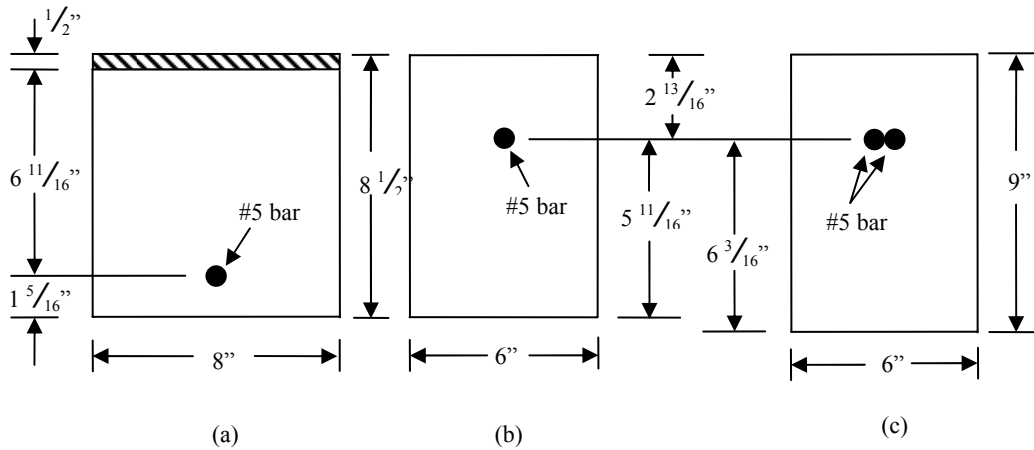


Figure 2. Illustration. Michael Baker, Inc. Design Cross Sections

As with the previous example, the ease of construction influences the amount and spacing of the reinforcing steel per cross section width. This leads to more conservative designs with higher moment capacities. The nominal transverse moment capacities for the Michael Baker, Inc. design cross sections are listed in Table 4.

Table 4. Nominal Moment Capacity of Michael Baker, Inc. Deck Design

Region	Per cross section width	Per 2 foot width
Positive bending between interior girders	9.84 k-ft per 8 inches	29.52 k-ft
Negative bending over interior girders	8.11 k-ft per 6 inches	32.44 k-ft
Negative bending in overhang	16.35 k-ft per 6 inches	65.40 k-ft

The nominal moment capacities from Tables 3 and 4 give a range of values which are typical of traditional reinforced concrete decks. These values serve as a benchmark to compare with the transverse moment capacities of the UHPC deck element of this report.

1.3 REPORT OUTLINE

This report is organized by first presenting an introduction along with typical reinforced concrete deck cross section designs in Chapter 1. Chapter 2 gives a review on flexural behavior of conventional concrete and then presenting the design methodology used for UHPC. Chapter 3 details the procedure for determining live and dead loads on the bridge deck panel. Chapter 4 uses the design methodology presented in Chapter 2 to analyze the flexural capacity of the bridge deck element. Finally an overview of the design loads and flexural capacities are presented in Chapter 5 with some closing remarks.

CHAPTER 2. UHPC FLUXURAL STRENGTH ANALYSIS METHODOLOGY

The following chapter compares the flexural behavior of conventional concrete and UHPC. The flexural behavior of prestressed concrete is briefly discussed to help explain the methodology for determining UHPC flexural capacity. The concept for analysis is given for a rectangular cross section containing prestressing strand as the only flexural reinforcement. Although concrete cross sections are not always rectangular, the basic principles discussed can be applied to more complex shapes with proper modifications to the given equations as long as equilibrium and strain compatibility are satisfied.

2.1 PRESTRESSED CONCRETE FLEXURAL BEHAVIOR

A prestressed concrete rectangular beam as illustrated in Figure 3a subjected to flexural bending well beyond its tensile cracking strength will develop a stress distribution as shown in Figure 3b. For this limit state, the concrete section is assumed to carry no tensile capacity. The only forces which develop within the cross section are from the concrete compression zone and the tensile resistance of the prestressing strands. Generally the stress distribution in Figure 3b is simplified as shown in Figure 3c, for analysis purposes, with a rectangular stress block having a magnitude of $\alpha_1 f_c'$, where f_c' is the concrete 28-day compressive strength and α_1 is typically taken as 0.85. The height of the stress block is taken as $a = \beta_1 c$, where c is the distance to the neutral axis measured from the top of the cross section and β_1 is a factor ranging between 0.65 to 0.85 (depending on f_c'). The resultant forces acting on the cross section from an idealized compressive stress distribution and steel stresses are illustrated in Figure 3d.

Figure 3e depicts the strain on the cross section at ultimate load for positive bending. The concrete above the neutral axis is in negative strain while the section below the neutral axis experiences positive strain. The steel strain, ϵ_{ps} , in Figure 3e is shown with respect to its own origin to depict the imposed prestress strain prior to casting.

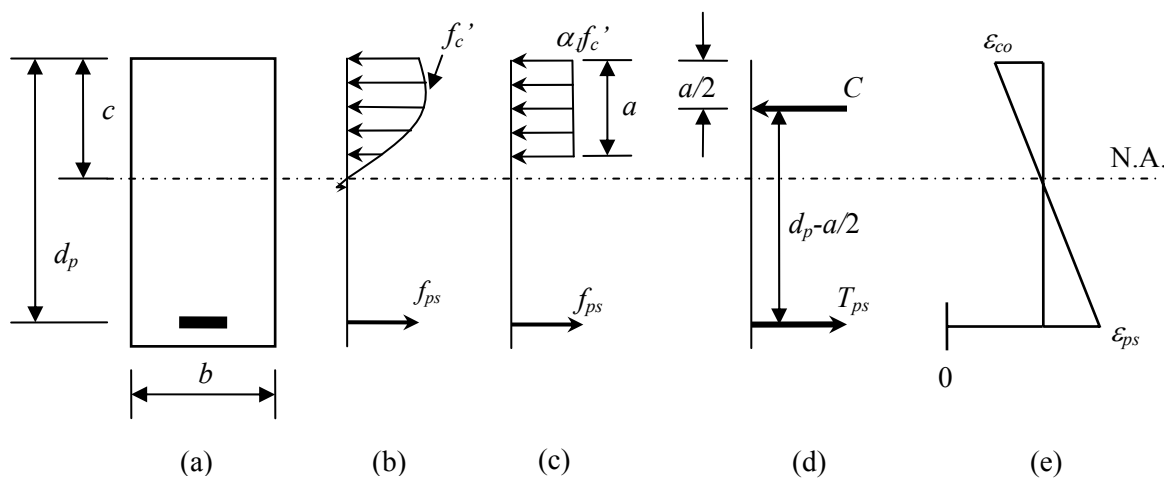


Figure 3. Illustration. Prestressed Concrete Internal Stress Behavior

The nominal moment capacity for the prestressed concrete beam is determined when both equilibrium and strain compatibility are satisfied for the cross section. Internal compressive and tensile forces must equate to each other. The compressive force is computed by equation (1) where b is the width of the cross section and other terms have previously been defined.

$$C = 0.85 f'_c ab \quad (1)$$

The tensile force is given by equation (2) where A_p is the area of the prestressing strands and f_{ps} is the tensile stress in the strands. The stress in the strand is dependent on both the existing prestress strain prior to casting and strain required to achieve equilibrium within the concrete cross section at ultimate load. The total steel strain is determined from a stress-strain analysis.

$$T_{ps} = A_p f_{ps} \quad (2)$$

The procedure to determine the nominal moment capacity of a beam usually requires an iterative process and an assumed method of failure. Typically the prestressing strands are assumed to have yielded while the concrete is at its maximum compressive stress, f'_c , and corresponding strain, ϵ_{co} , of 0.003 for normal concrete. The height of the stress block, a , is assumed and a value for c is determined by dividing a by β_1 . A strain compatibility analysis on the cross section is performed to determine the strain in the prestressing strand, ϵ_{ps} . Total strain in the strand is comprised of the effective prestress strain, ϵ_{pe} , decompression strain, ϵ_2 , and the strain required to develop nominal moment capacity, ϵ_3 . The effective prestress strain, ϵ_{pe} , is given by equation (3) where f_{pe} is the effective prestress and E_{ps} is the modulus of elasticity in the strands.

$$\epsilon_{pe} = \frac{f_{pe}}{E_{ps}} \quad (3)$$

Decompression strain, ϵ_2 , is computed with equation (4) where P_e is the effective prestress force, A_c is the area of the concrete cross section, E_c is the concrete modulus of elasticity, M is the moment produced from the eccentric force from the prestressing strands, y is the distance between the cross section centroidal axis to the strands, and I is the moment of inertia of the cross section.

$$\epsilon_2 = \frac{P_e}{A_c E_c} + \frac{My}{IE_c} \quad (4)$$

The strain required to develop nominal moment capacity, ϵ_3 , is given by equation (5) where d_p is the depth of the tendon measured from the top surface of the beam.

$$\epsilon_3 = \frac{d_p - c}{c} \epsilon_{co} \quad (5)$$

The sums of these three strains (ϵ_3 can be positive or negative depending on the type of bending) correspond to a steel stress and thus a force, $A_p f_{ps}$, in the strand.

The assumed value for the stress block height, a , can then be checked with the calculated steel force from the stress-strain analysis as shown in equation (6).

$$a = \frac{A_p f_{ps}}{0.85 f'_c b} \quad (6)$$

If this computed value is not relatively close to the assumed value, then the process should be repeated with a new value for a . The value generated from equation (6) is a good assumption for the next iteration. This process may take three to four iterations to arrive at acceptable values for a and c .

Once the neutral axis is established, the compressive (equation (1)) and tensile (equation (2)) forces are calculated to verify they are equal to each other. With both equilibrium and strain compatibility satisfied, the nominal moment capacity for the beam is computed by taking a moment about the centroid of the compression stress block as expressed by equation (7).

$$M_n = T_{ps} \left(d_p - \frac{a}{2} \right) \quad (7)$$

Although the presented equations are for a generic rectangular cross section, these basic principles can be applied to other cross sections by appropriately modifying the preceding equations provided equilibrium and strain compatibility are not violated.

2.2 PRESTRESSED UHPC FLEXURAL BEHAVIOR

The uniaxial stress-strain behavior of UHPC differs from conventional concrete in several ways. Most notably, UHPC exhibits tensile capacity well past initial tensile cracking. Tensile capacity is maintained until pullout of the fiber reinforcement occurs at strain levels approaching 0.01.⁽²⁾ Additionally, as compared to the compressive stress-strain response of conventional concrete, UHPC exhibits a significantly more linear load-deformation response up through compressive failure. Finally, UHPC exhibits a very high compressive strength, approximately 28 ksi, as compared to conventional and high performance concretes. An approximate UHPC uniaxial stress-strain curve developed from a previous study on UHPC prestressed I-girders is shown by the broken line in Figure 4.^(2,8)

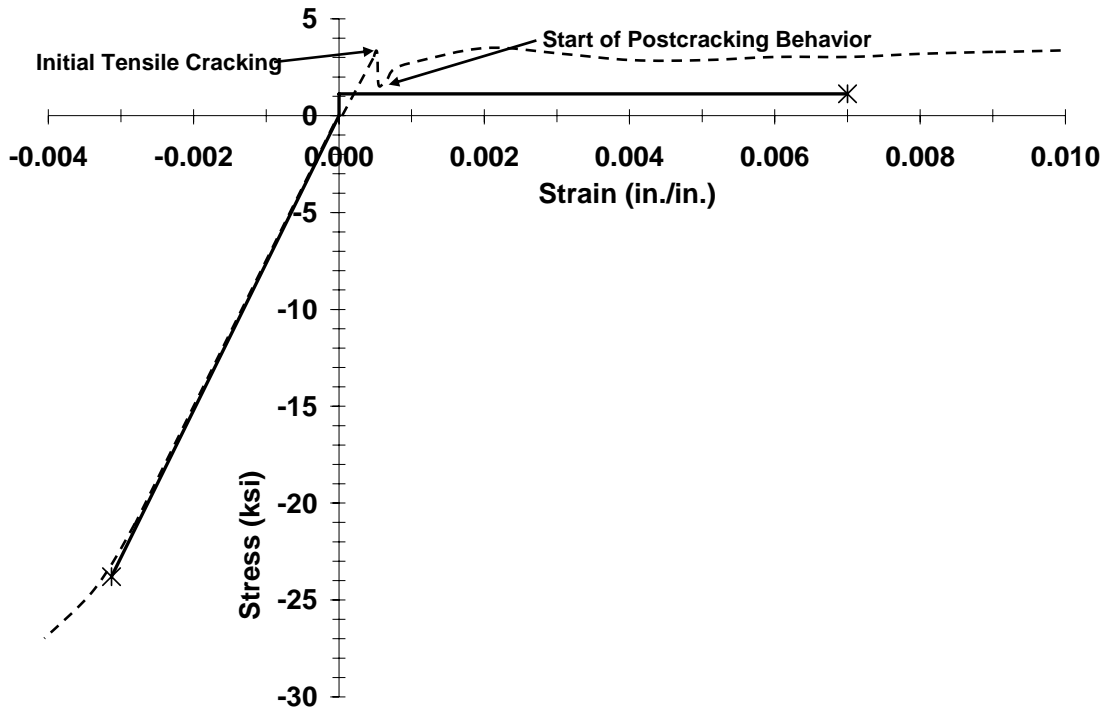


Figure 4. Graph. Experimental and Simplified UHPC Uniaxial Stress-Strain Behavior

Given the experimentally defined UHPC stress-strain curve, a more practical and conservative UHPC stress-strain relationship can be developed for design purposes. First, in order to take advantage of the tensile capacity of UHPC, a tensile behavior model with some tensile capacity after cracking must be stipulated. This model needs to include the shape of the tensile response, the stress level of the tensile response, f_{mt} , and the limiting tensile strain, ϵ_{mt} , prior to impending fiber pullout. For this analysis a limiting tensile strain, ϵ_{mt} , of 0.007 is anticipated to be conservative based on current experience with prestressed UHPC members. To simplify the modeling of the behavior of UHPC in tension, the tensile behavior can be modeled as rigid-perfectly plastic from zero strain through fiber pullout. As compared to the experimentally observed tensile stress-strain behavior shown in Figure 4, the proposed model is only unconservative over a small strain range during initial tension and is quite conservative over the remainder of the tensile strain range. Finally, the limiting tensile capacity, f_{mt} , for the UHPC is defined. In the current model, it is taken as 75% of 1.5 ksi, with 1.5 ksi being the suggested UHPC tensile strength, f_t^* , from a prior structural behavior study.⁽²⁾ Thus, f_{mt} for the model in this report is taken as $(0.75)1.5$ ksi.

Compression tests on cylinders from the UHPC material characterization study have shown the modulus of elasticity to be about 7600 ksi and the compressive strength, f_c' , to be 28 ksi.⁽¹⁾ For design purposes, the UHPC compressive strength is assumed to be limited to 85% of f_c' and thus the limiting compressive strength, f_{mc} , for the model is 23.8 ksi. Experimental observations have demonstrated the UHPC compressive stress-strain response to be within 5% of linear elastic behavior up to about 80 and 90% of its compressive strength, thus, assuming linear elastic behavior through the limiting compressive strength is reasonable.⁽¹⁾ The limiting compressive

strain, ε_{mc} , for the model is f_{mc} divided by the modulus of elasticity, or 0.003132. The idealized UHPC stress-strain relationship just described is depicted by the solid line in Figure 4.

This UHPC bending behavior model can thus be applied to beam design. A rectangular prestressed UHPC beam as shown in Figure 5a loaded to the compressive and tensile strain limits (i.e. an impending balanced failure of the UHPC) would develop the generalized internal stress distribution shown in Figure 5b. This stress distribution is comparable to the experimentally defined stress-strain curve in Figure 4. For a conservative and simple analysis of the beam, the idealized stress-strain model previously described and illustrated by the solid line in Figure 4 is employed. The simplified stress distribution is shown in Figure 5c.

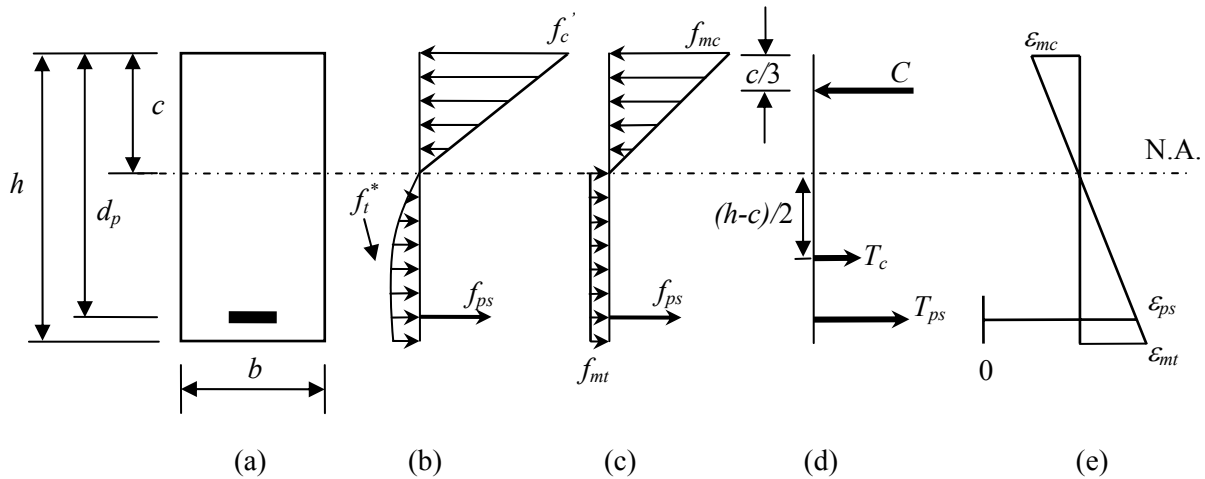


Figure 5. Illustration. Prestressed UHPC Internal Stress Behavior

The UHPC compressive force is approximated by a triangular stress distribution and expressed according to equation (8). The limiting compressive strength, f_{mc} , for the design example of this report is taken as $0.85f'_c$. The resultant of the compressive force, C , can be taken as acting at one-third the neutral axis depth below the extreme compression fiber of the beam.

$$C = \frac{1}{2} f_{mc} cb \quad (8)$$

A uniform tensile stress of f_{mt} acting from the neutral axis to the extreme tension fiber is used to approximate the UHPC tensile force as shown in equation (9), where h is the overall height of the beam.

$$T_c = f_{mt} (h - c)b \quad (9)$$

The tensile force from the prestress tendons is expressed in the same manner as for normal prestressed concrete (equation (2)). Figure 5d illustrates the three primary forces present within the cross section in bending, namely the concrete compressive force, C , the concrete tensile force, T_c , and the prestressing steel force, T_{ps} .

Determining the moment capacity for a UHPC beam is a more involved process than for traditional prestressed concrete beams. The analysis of the normal prestressed concrete beam typically assumes the concrete to be in at state of compressive strain corresponding to impending concrete crushing and the prestressing strands to be near yielding. The moment capacity of UHPC on the other hand could be limited by either the compressive strain, ε_{mc} , associated with f_{mc} , or the tensile strain, ε_{mt} , associated with f_{mt} . An outlined process to determine moment capacity is illustrated in Figure 6.

As a preliminary step, the geometric dimensions and properties of the cross section should be defined. Additionally, the limiting strains and strengths (i.e. ε_{mc} , ε_{mt} , f_{mc} , f_{mt}) for the UHPC model should be established. Once an effective prestress is determined, the effective strain, ε_{pe} , and decompression strain, ε_2 , for the prestress strands can be determined by equations (3) and (4). As an aid during the iterative process, the neutral axis for a balanced UHPC compressive and tensile failure is computed by equations (10) and (11). Equation (10) is used when the member is subjected to positive bending while equation (11) is for negative bending.

$$c_{b+} = \frac{\varepsilon_{mc}}{\varepsilon_{mc} + \varepsilon_{mt}} h \quad (10)$$

$$c_{b-} = \frac{\varepsilon_{mt}}{\varepsilon_{mc} + \varepsilon_{mt}} h \quad (11)$$

After the preliminary items have been defined, a value for the neutral axis, c , is assumed. This value of c is checked against c_b to determine the state of the UHPC (e.g. impending UHPC crushing or tension loss due to fiber pullout) during the strain analysis. In positive bending, if c is less than c_{b+} then the UHPC has reached the limiting tensile strain, ε_{mt} , and the compressive strain, ε_c , must be determined from a strain analysis. On the other hand, if c is greater than c_{b+} , then the UHPC is at the limiting compressive strain, ε_{mc} , and the tensile strain, ε_t , must be determined from a strain analysis. Once it has been established which strains are present along the cross section, appropriate compressive and tensile stresses can be determined for the current iterative step. It should be noted that the UHPC tensile stress, f_t , is equal to f_{mt} for tension strains between the neutral axis and ε_{mt} while the general UHPC compressive stress, f_c , varies linearly for compressive strains between the neutral axis and ε_{mc} . The strain in the prestressing strands, ε_3 , is determined from the strain analysis. This value is added to the other steel strains to compute the total strand stress.

Knowing the UHPC compressive and tensile stresses and the strand tensile stresses, the internal forces can be calculated with equations (8), (9), and (2). The next step is to verify the cross section is in equilibrium by comparing the total compressive force to the total tensile force. If these forces are not approximately equal to each other, then a new value for c is assumed and the procedure is repeated. As guidance, a value for c can be calculated from equation (12) where all the terms have been previously defined and all values coincide with the current iteration of the analysis.

$$c = \frac{A_p f_{ps} + f_{mt} h b}{b \left(\frac{1}{2} f_{mc} + f_{mt} \right)} \quad (12)$$

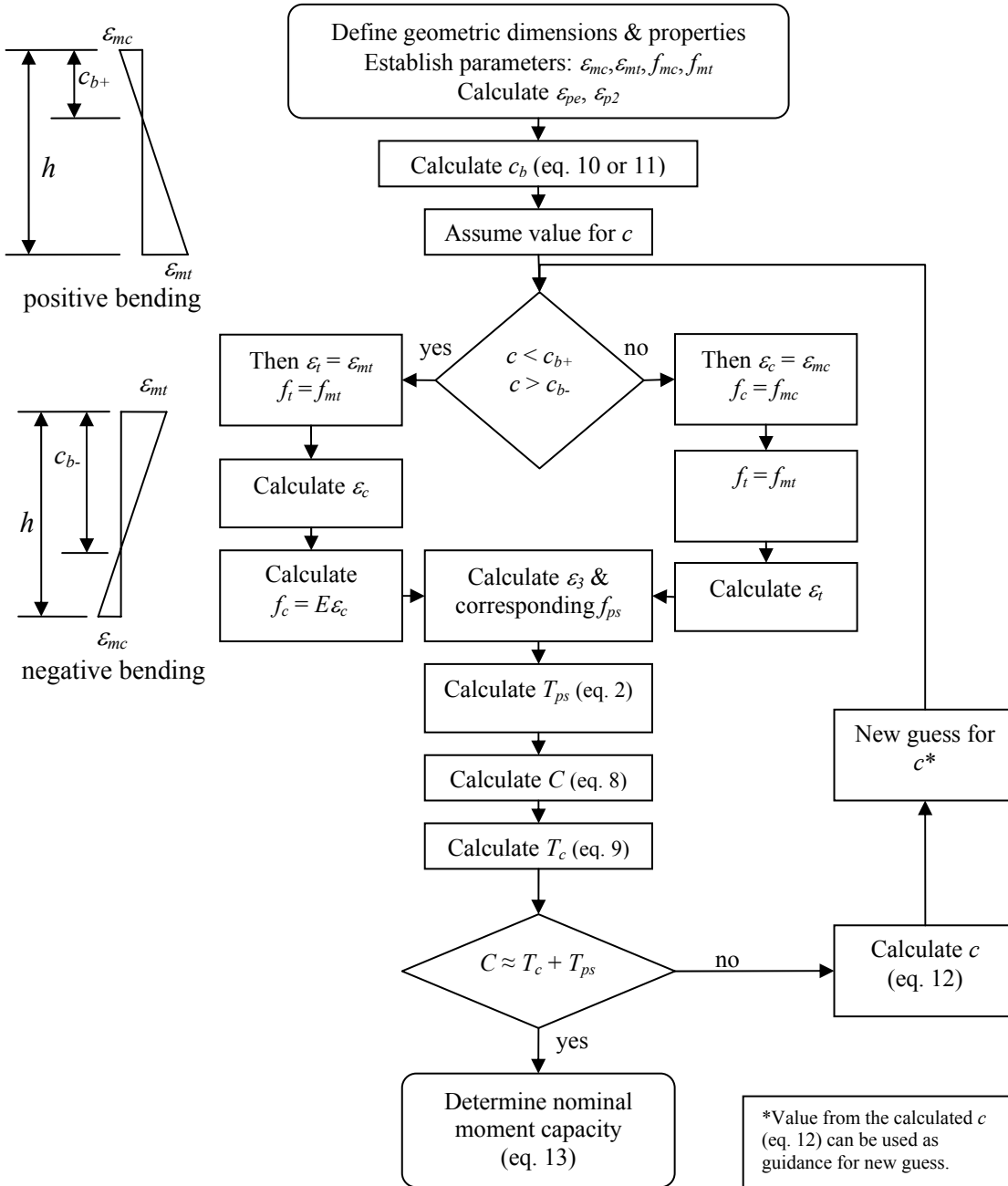


Figure 6. Illustration. Flowchart for Determining Moment Capacity for UHPC Beams

Once an acceptable value for c has been obtained, the nominal moment capacity of the beam is determined with equation (13). The moment for this equation is taken about the compressive force resultant of the UHPC.

$$M_n = T_{ps} \left(d_p - \frac{c}{3} \right) + T_c \left(\frac{h}{2} + \frac{c}{6} \right) \quad (13)$$

The steps detailed in this section of the report are for computing the nominal positive moment capacity of a prestressed rectangular UHPC cross section. Similar steps can be followed to determine the negative moment capacity of a member by modifying equations (8), (9), (12), and (13). Additionally, these basic principles can be extended to other cross sections. Care should be taken during the analysis to ensure strain compatibility and equilibrium are not violated. An example of a detailed positive and negative moment capacity analysis of a T-beam cross section is provided in Chapter 4.

CHAPTER 3. UHPC DECK SLAB DESIGN LOADS

The following chapter discusses the procedure used to determine live, dead, and collision loads on the UHPC deck for different limit states. The 2006 AASHTO LRFD Bridge Design Specifications have been used to determine the appropriate loads.

Design of the UHPC two-way ribbed deck first consists of defining an element with all appropriate dimensions. Positive, negative, and overhang collision moments are calculated from the given parameters of the system. Once moments for the different limit states are calculated, the UHPC cross section is analyzed to determine the nominal moment capacity.

3.1 DECK SLAB PARAMETERS

The precast, prestressed UHPC two-way ribbed deck is composed of a flat plate on a series of longitudinal and transverse webs. Webs are spaced at 2-foot centers in both directions. For this example, deck panels are 38 feet wide in the transverse direction and 8 feet in the longitudinal direction. This panel width allows for two 12-foot wide lanes of traffic plus shoulders. At this point within the development of this conceptual design, the transverse joints are assumed to be connected together with post-tensioning and a grouted shear key. In this example, support for the UHPC deck panels is provided by five AASHTO Type IV concrete girders evenly spaced at 8 feet. Composite action between the girders and the deck is assured via shear connectors that extend from the girders into the pockets formed by the intersecting webs of the deck panel. These pockets are grouted after all adjacent panels have been connected and secured together. The railing for this example is a Type-F concrete parapet. Figure 7 is a schematic of the plan and cross section view of the UHPC deck system.

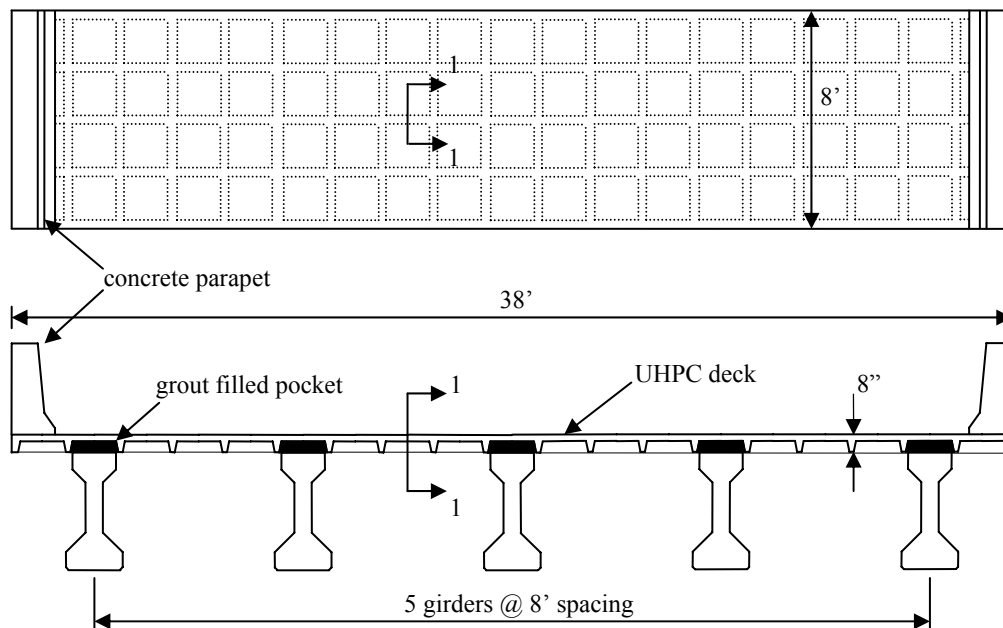


Figure 7. Illustration. UHPC Bridge Deck Panel Plan and Cross Section View

3.1.1 T-Beam Cross Section

For analysis, a T-beam cross section with an effective flange width of 24 inches is used. This effective flange width is based on Section 4.6.2.6 of the AASHTO LRFD Bridge Design Specifications which is used as guidance due to the lack of formal design specifications for UHPC. The overall thickness of the precast deck panel is 8 inches (from top surface to bottom of web) and is within the limits set in AASHTO LRFD Bridge Design Specifications Section 9.7.5 for concrete precast deck slabs. However, the overhang of the exterior longitudinal web is at the thickness limit set for traditional concrete overhangs in AASHTO LRFD Bridge Design Specifications Section 13.7.3.1.2. It should be noted that the T-beam cross section is not thickened in the overhang region, as UHPC has a higher compressive strength and a useable tensile capacity thus reducing the need for additional material in this region.

The resulting transverse cross section is shown in Figure 8 and is Section 1-1 with respect to Figure 7. Deck thickness is 2.75 inches (used for dead load calculations) of which only 2.5 inches are considered for strength calculations. The top quarter inch of the deck element may be marred and irregular as a result of the casting process and thus is disregarded. The web forming the T-section is 3 inches thick and 5.5 inches tall. The web has a slight taper that is ignored when computing the moment capacity. The overall height of the deck is 8 inches. Dimensions for Figure 8 are listed in Table 5.

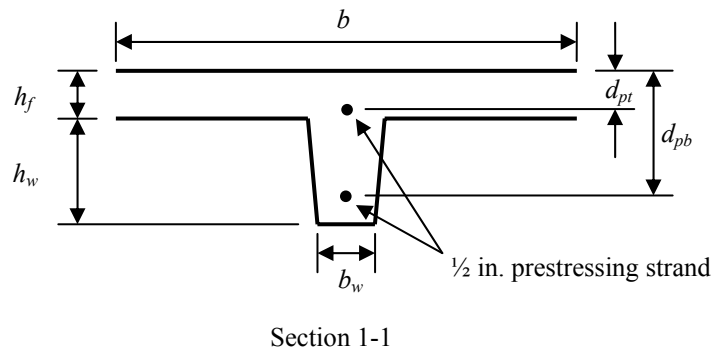


Figure 8. Illustration. UHPC Transverse Strip Cross Section

Table 5. T-Beam Dimensions

Property	Dimension
Effective width, b	24 in.
Flange thickness, h_f	2 ½ in.
Web height, h_w	5 ½ in.
Web width, b_w	3 in.
Top strand depth, d_{pt}	2 in.
Bottom strand depth, d_{pb}	6 ½ in.

3.1.2 Material Properties

The material properties for the components of the UHPC deck panel along with the parameters for the UHPC flexural model are listed in Table 6. Values for the UHPC unit weight and flexural behavior model, (i.e., compressive strength, compressive strain, tensile strength, and tensile strain) are based on a previous material characterization study.⁽¹⁾ Prestressing for the element are ½ inch diameter 270 ksi low-relaxation strands.

Table 6. Material Properties and UHPC Limiting Parameters

Property	Value
UHPC unit weight	156 lb/ft ³
UHPC limiting compressive strength, f_{mc}	23.8 ksi
UHPC modulus of elasticity, E	7600 ksi
UHPC limiting compressive strain, ϵ_{mc}	0.003132 in./in.
UHPC sustainable tensile strength, f_{mt}	1.125 ksi
UHPC limiting tensile strain, ϵ_{mt}	0.007 in./in.
prestressing strand ultimate strength, f_{pu}	270 ksi
wearing surface unit weight	140 lb/ft ³

3.1.3 Concrete Parapet Properties

In this design example, a Type-F concrete railing will be used for the analysis. UHPC deck panels could also be analyzed by using a post and beam railing, which is usually lighter, if dead weight is a limiting criterion. Properties for the Type-F parapet are shown in Table 7.

Table 7. Type-F Concrete Parapet Properties

Property	Value
Weight per unit length	650 lb/ft
Collision moment capacity, M_c	17.83 kip-ft/ft
Transverse resistance of railing, R_w	137.22 kip
Critical length of yield line failure pattern, L_c	235.2 in.
Parapet height, H	42 in.
Width at base of parapet	20.25 in.
Center of gravity, measured from exterior face	7.61 in.

3.2 METHOD OF DETERMINING DESIGN LOADS

Design loads are based on the cross section of Figure 8 and the values in Tables 5, 6, and 7. Design moments are determined for three different regions along the T-beam cross section. These regions are for the span between girders, sections over interior girders, and the overhang section. Interior bays between girders are investigated for positive bending at the Strength I limit state. Sections over interior girders are examined for negative bending at the Strength I limit

state. The overhang region is investigated for different combinations of dead, live, and collision load for the Strength I and Extreme Event II limit state. Load factors for the three different regions and accompanying limit states are presented in Table 4 and taken from Section 3.4 and A13.4 of the AASHTO LRFD Bridge Design Specifications.

Table 8. Load Combinations and Load Factor

Region	Limit State	DC	DW	LL
Between interior girders	Strength I	1.25	1.50	1.75
Over interior girders	Strength I	1.25	1.50	1.75
Overhang	Strength I	1.25	1.50	1.75
Overhang	Extreme Event II	1.00	1.00	1.75

Note: **DC** – dead load of structural components
DW – dead load of wearing surface
LL – vehicular live load

3.3 INTERIOR DECK DESIGN LOADS

Loads for positive and negative bending for the interior deck are designed for Strength I limit state. Dead loads for this region are due to the UHPC and the wearing surface. For moment capacity analysis, the web width is taken as 3 inches but the actual component tapers upward. A web width of 3.5 inches is used to account for the slight taper for dead weight calculations. For dead load, the flange height is taken to be 2.75 inches as previously noted. Additionally, the 2-foot spaced longitudinal webs add to the cross section dead load and will be evenly distributed over the transverse length of the deck. The resulting dead loads are as follows.

UHPC:

$$w_{uhpc} = 0.156 \text{ kpf} \left((24 \text{ in})(2.75 \text{ in}) + (3.5 \text{ in})(5.5 \text{ in}) + \frac{(20.5 \text{ in})(5.5 \text{ in})(3.5 \text{ in})}{24 \text{ in}} \right) \left(\frac{1 \text{ ft}^2}{144 \text{ in}^2} \right)$$

$$w_{uhpc} = 0.110 \frac{\text{kip}}{\text{ft}}$$

Wearing surface:

$$w_{ws} = 0.140 \text{ kpf} \left((24 \text{ in})(2.5 \text{ in}) \right) \left(\frac{1 \text{ ft}^2}{144 \text{ in}^2} \right) = 0.058 \frac{\text{kip}}{\text{ft}}$$

Factored dead load:

$$w_{DLU} = (1.25) \left(0.110 \frac{\text{kip}}{\text{ft}} \right) + (1.50) \left(0.058 \frac{\text{kip}}{\text{ft}} \right) = 0.225 \frac{\text{kip}}{\text{ft}}$$

The moment caused from the factored dead load is approximated by using equation (14) where w is the distributed load, and l is the span length.

$$M = \frac{wl^2}{10} \quad (14)$$

Factored dead load moment:

$$M_{DLU} = \frac{\left(0.225 \frac{\text{kip}}{\text{ft}}\right)(8\text{ft})^2}{10} = 1.440\text{kipft}$$

3.3.1 Positive Moment

A simplified approach was employed for determining the maximum positive design moment. Table A4-1 from the AASHTO LRFD Bridge Design Specifications lists the maximum positive live load moment to be 5.69 kip-ft per width for beams spaced at 8 feet. It should be noted that the values in Table A4-1 from the AASHTO LRFD Bridge Design Specifications account for multiple presence factors and dynamic load allowances. For a 2-foot width, which is the T-beam cross section width, this equates to a live load moment of 11.38 kip-ft. The live load moment is factored and added to the factored dead load moment to get the positive design moment for the interior of the deck panels.

Interior panel positive moment:

$$M_{U+} = 1.440\text{kipft} + (1.75)(11.38\text{kipft}) = \underline{\underline{21.36\text{kipft}}}$$

3.3.2 Negative Moment

Table A4-1 from the AASHTO LRFD Bridge Design Specifications is also used to determine the negative moment over interior beams. First the location of the design section for negative moment is determined to find the appropriate value from Table A4-1. AASHTO LRFD Bridge Design Specification Section 4.6.2.1.6 specifies the location of the design section. The design section is dependent on the flange width of the AASHTO type IV beam. AASHTO type IV beams have a flange width of 20 inches and thus the design section is computed as shown below.

Design section:

$$x_{sect} = \frac{1}{3}(20\text{in}) = 6.667\text{in}$$

The listed negative moment for beam spacing of 8 feet and design section of 6 inches (rounded down for a conservative value) is 4.81 kip-ft. For a 2-foot width, this translates to 9.62 kip-ft. Therefore the negative moment over interior girders is added to the factored dead load moment and computed as follows.

Interior girder negative moment:

$$M_{U-} = 1.440 \text{kip ft} + (1.75)(9.62 \text{kipft}) = \underline{\underline{18.28 \text{kipft}}}$$

3.4 OVERHANG DESIGN LOADS

Negative moments for the overhang region require investigation of several design cases and regions between the interior face of the parapet and the design section towards the interior side of the exterior girder. Each design case is described in the following sections. The design section (i.e. 6.67 inches from the centerline of the exterior girder) used in the overhang analysis is the same value as calculated in section 3.3.2 of this report. AASHTO LRFD Bridge Design Specification Section A13.4 is used as guidance for the different design cases of the overhang. Cross sections for investigation are shown in Figure 9. A distribution angle of 30° is used to distribute the collision force and moment capacity of the parapet to the different cross sections in the overhang region as will be presented in upcoming sections of this report.

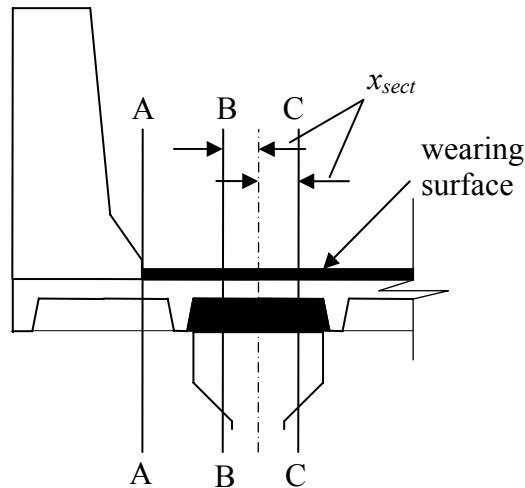


Figure 9. Illustration. Sections for the Overhang Region

3.4.1 Design Case I: Transverse and Longitudinal Collision Forces

Design Case I accounts for the transverse and longitudinal forces experienced from a collision on the parapet and the dead load of the structure. This is an Extreme Event II limit state and the appropriate load factors are given in Table 8. Three different cross sections are examined for this case. They are A-A at the interior face of the parapet, B-B towards the exterior of the panel measured from the centerline of the exterior girder, and C-C towards the interior of the panel measured from the centerline of the exterior girder.

3.4.1.1 Section at Face of Parapet (Section A-A)

Loads acting on cross section A-A of the overhang consist of the parapet, UHPC deck, collision moment capacity of the railing, and the transverse load resistance of the parapet. The letter P in Figure 10 denotes the center of gravity for the parapet. The moment at section A-A is modeled by a cantilever beam with an applied uniform load from the T-beam section and a point load acting at the edge due to the exterior web. Recall that h_f is taken as 2.75 inches and thus the cross sectional area of the T-beam is 85.25 in^2 or 0.592 ft^2 . The width of the exterior web is taken as 3.5 inches and has a cross sectional area of 112.75 in^2 or 0.783 ft^2 . Moments at cross section A-A from self-weights of the structural components are shown below.

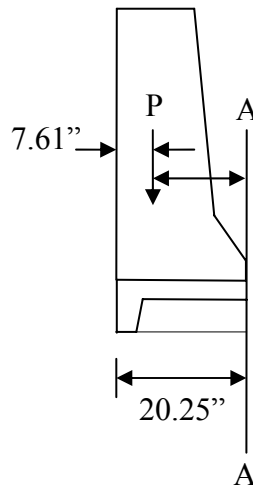


Figure 10. Illustration. Section A-A of the Overhang

Moment at A-A from T-beam:

$$M_{A-A:T} = \frac{(0.592\text{ft}^2)(0.156\text{kcf})(1.6875\text{ft})^2}{2} = 0.131\text{kipft}$$

Moment at A-A from exterior web:

$$M_{A-A:ex-web} = (0.783\text{ft}^2)(0.292\text{ft})(0.156\text{kcf})(1.542\text{ft}) = 0.055\text{kipft}$$

Moment at A-A from parapet:

$$M_{A-A:par} = 0.650 \frac{\text{kip}}{\text{ft}} (2\text{ft})(1.053\text{ft}) = 1.369\text{kipft}$$

The collision capacity moment of the parapet is dispersed with a distribution angle if the section investigated is away from the face of the parapet. Additionally it is assumed the moments and tension forces resulting from a collision are effectively transmitted and distributed between

adjacent UHPC panels. For section A-A, distribution is not necessary since the section is at the face of the parapet.

Collision moment at A-A:

$$M_{A-A:coll} = \frac{(17.83 \text{kipft / ft})(19.6 \text{ft})}{19.6 \text{ft}} (2 \text{ft}) = 35.66 \text{kipft}$$

The total negative moment for section A-A is the sum of the moments just calculated with appropriate load combinations.

Factored negative moment at A-A:

$$M_{A-A} = 1.00(0.131 \text{kipft} + 0.055 \text{kipft} + 1.369 \text{kipft}) + 35.66 \text{kipft} = \underline{\underline{37.22 \text{kipft}}}$$

In addition to the collision moment capacity of the parapet, the deck panel must resist the transverse resistance of the railing. This force propagates through the face of the parapet by way of a yield line failure mechanism. Section A13.4.2 of the AASHTO LRFD Bridge Design Specification denotes the tensile force as shown in equation (15) where R_w is the total transverse resistance of the railing, L_c is the critical length of the yield line failure, and H is the height of the railing.

$$T = \frac{R_w}{L_c + 2H} \quad (15)$$

The maximum tensile force which must be resisted at section A-A per linear foot is the following.

$$T_{A-A:coll} = \frac{137.22 \text{kip}}{19.6 \text{ft} + (2)(3.5 \text{ft})} = 5.159 \frac{\text{kip}}{\text{ft}}$$

Recalling the width of the T-beam cross section is 2 feet, the total design tensile force is the following.

$$T_{A-A} = (2 \text{ft}) \left(5.159 \frac{\text{kip}}{\text{ft}} \right) = \underline{\underline{10.32 \text{kip}}}$$

For Design Case I at cross section A-A, the design moment and tensile force which must be resisted are shown below.

$$M_{A-A} = 37.22 \text{ kip ft} \quad T_{A-A} = 10.32 \text{ kip}$$

3.4.1.2 Design Section Towards Exterior of Deck (Section B-B)

Loads acting on cross section B-B of the overhang consist of the parapet, UHPC deck, wearing surface, collision moment capacity of the railing, and the transverse load resistance of the parapet. The moment caused by the self-weight of the UHPC deck element is modeled as a distributed load from the T-beam, a point load from the exterior edge web, and a point load from the first interior web. Figure 11 illustrates the structural components and dimensions needed to determine dead load moments. Recalling from section 3.4.1.1 of this report, the T-beam cross sectional area is 85.25 in² and the edge web cross sectional area is 112.75 in². The cross sectional area for the first interior web is taken as 112.75 in². The thickness of the wearing surface is 2.5 inches and thus yields a cross sectional area of 60 in² over the 2 foot section. Unfactored moments due to the structural components are shown below.

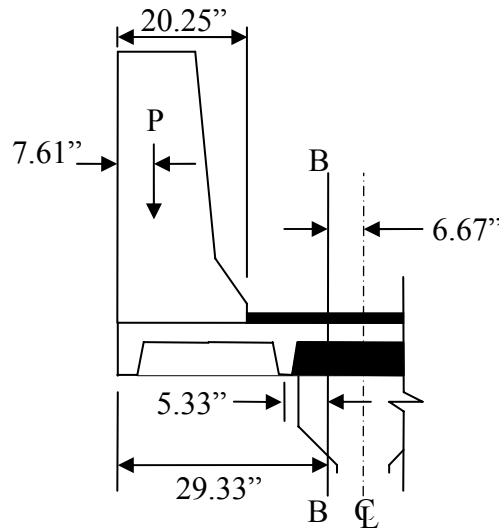


Figure 11. Illustration. Section B-B of the Overhang

Moment at B-B from T-beam:

$$M_{B-B:T} = \frac{(0.592\text{ft}^2)(0.156\text{kcf})(2.444\text{ft})^2}{2} = 0.276\text{kipft}$$

Moment at B-B from exterior web:

$$M_{B-B:ex-web} = (0.783\text{ft}^2)(0.292\text{ft})(0.156\text{kcf})(2.298\text{ft}) = 0.082\text{kipft}$$

Moment at B-B from first interior web:

$$M_{B-B:in-web} = (0.783\text{ft}^2)(0.292\text{ft})(0.156\text{kcf})(0.444\text{ft}) = 0.016\text{kipft}$$

Moment at B-B from parapet:

$$M_{B-B:par} = 0.650 \frac{\text{kip}}{\text{ft}} (2\text{ft})(1.810\text{ft}) = 2.353\text{kipft}$$

Moment at B-B from wearing surface:

$$M_{B-B:ws} = \frac{(0.417\text{ft}^2)(0.140\text{kcf})(0.757\text{ft})^2}{2} = 0.017\text{kipft}$$

Since cross section B-B is a distance away from the parapet face, the collision moment capacity is assumed to evenly disperse over a length equal to L_c and 2 times $x \tan \theta$ as illustrated in Figure 12.

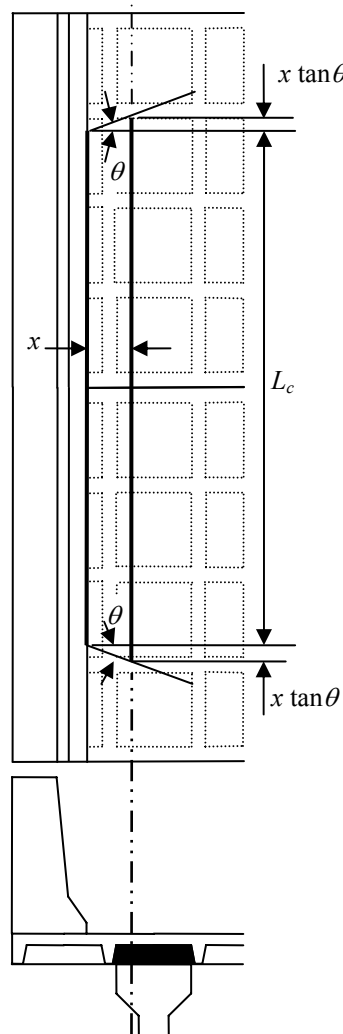


Figure 12. Illustration. Distribution of Collision Moment

The total collision moment capacity of the parapet is first computed for the critical yield line failure length and then distributed over the propagated length. This value is then adjusted to reflect a 2-foot width cross section as shown in the following calculation.

Collision moment at B-B:

$$M_{B-B:coll} = \frac{(17.83 \text{kipft/ft})(19.6 \text{ft})}{19.6 \text{ft} + (2)(0.757 \text{ft})(\tan 30^\circ)} (2 \text{ft}) = 34.138 \text{kipft}$$

Factored negative moment at B-B:

$$M_{B-B} = 1.00(0.276 \text{kipft} + 0.082 \text{kipft} + 0.016 \text{kipft} + 2.353 \text{kipft}) \\ + 1.00(0.017 \text{kipft}) + 34.138 \text{kipft} = \underline{\underline{36.88 \text{kipft}}}$$

The transverse collision force at section B-B is determined by modifying equation (15) and distributing the axial force over the distance, $L_c + 2H + 2x \tan \theta$.

Tensile collision force at B-B per linear foot:

$$T_{B-B:coll} = \frac{137.22 \text{kip}}{19.6 \text{ft} + (2)(3.5 \text{ft}) + (2)(0.757 \text{ft})(\tan 30^\circ)} = 4.995 \frac{\text{kip}}{\text{ft}}$$

Tensile collision force at B-B:

$$T_{B-B} = (2 \text{ft}) \left(4.995 \frac{\text{kip}}{\text{ft}} \right) = \underline{\underline{9.99 \text{kip}}}$$

For Design Case I at cross section B-B, the design moment and tensile force are the following.

$$M_{B-B} = 36.88 \text{ kip ft} \qquad T_{B-B} = 9.99 \text{ kip}$$

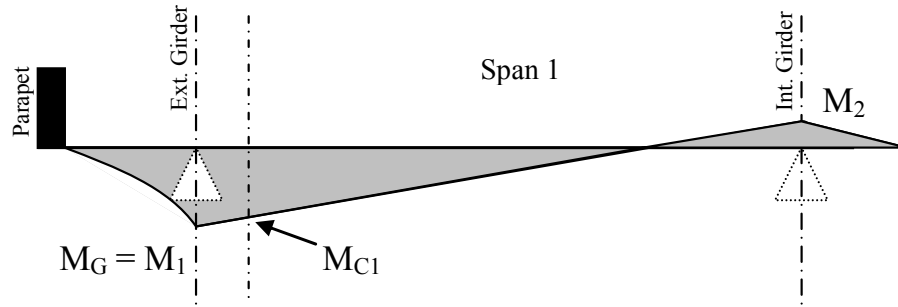


Figure 14. Illustration. Approximate Moment Diagram between Exterior Girder and First Interior Girder Due to Dead Loads on Overhang.

Moments from the dead loads on the overhang region are computed in the following steps.

Moment at centerline of exterior girder from T-beam:

$$M_{G:T} = \frac{(0.592\text{ft}^2)(0.156\text{kcf})(3\text{ft})^2}{2} = 0.416\text{kipft}$$

Moment at centerline of exterior girder from exterior web:

$$M_{G:web} = (0.783\text{ft}^2)(0.292\text{ft})(0.156\text{kcf})(2.854\text{ft}) = 0.102\text{kipft}$$

Moment at centerline of exterior girder from first interior web:

$$M_{G:web} = (0.783\text{ft}^2)(0.292\text{ft})(0.156\text{kcf})(1.0\text{ft}) = 0.036\text{kipft}$$

Moment at centerline of exterior girder from parapet:

$$M_{G:par} = 0.650 \frac{\text{kip}}{\text{ft}} (2\text{ft})(2.366\text{ft}) = 3.076\text{kipft}$$

Moment at centerline of exterior girder from wearing surface:

$$M_{G:ws} = \frac{(0.417\text{ft}^2)(0.140\text{kcf})(1.3125\text{ft})^2}{2} = 0.050\text{kipft}$$

Factored negative moment at centerline of exterior girder due to dead loads on the overhang:

$$M_G = 1.00(0.416\text{kipft} + 0.102\text{kipft} + 0.036\text{kipft} + 3.076\text{kipft}) \\ + 1.00(0.050\text{kipft}) = 3.680\text{kipft}$$

Given the factored negative moment at the centerline of the exterior girder, the deck span, and the assumed value of M_2/M_1 , a negative moment from the overhang loads can be determined for cross section C-C.

Factored negative moment at cross section C-C due to dead loads on the overhang:

$$M_{C-C:1} = 3.680 \text{kipft} \left(1 - \frac{1.4(0.556 \text{ft})}{8 \text{ft}} \right) = \underline{3.322 \text{kipft}}$$

Dead loads from interior spans influencing the moment on the first span consist of the UHPC deck and wearing surface. The dead load of the UHPC deck element is taken as a uniform distributed load. The uniform distributed load is comprised of the dead load of the T-beam cross section and the longitudinal webs which have been distributed over the span. The approximate moment diagram for span 1 from interior deck dead loads is shown in Figure 15.

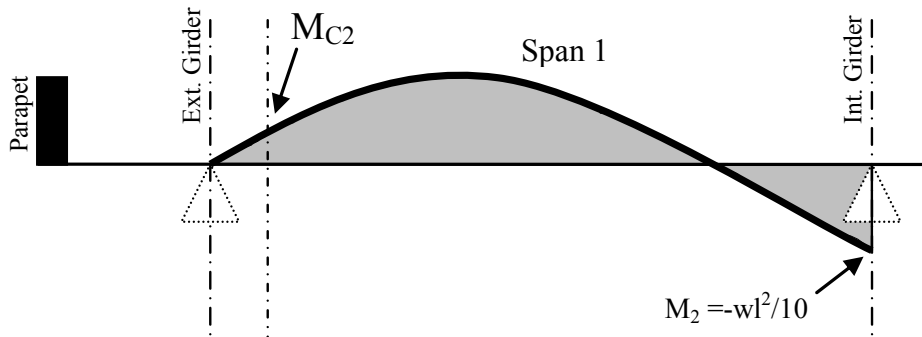


Figure 15. Illustration. Approximate Moment Diagram between Exterior Girder and First Interior Girder Due to Dead Loads on Interior Spans.

The shape of the moment diagram in Figure 15 can be derived by taking a free body diagram of span 1 and applying a uniform distributed load, w , and a moment of $wl^2/10$ at the first interior girder (typical of a continuous beam with one unrestrained end). Applying equations of equilibrium to the free body diagram, the shape of the moment diagram can be described by equation (16).

$$M = \frac{4wl}{10}x - \frac{wx^2}{2} \quad (16)$$

Recall from section 3.3, the UHPC and wearing surface uniform dead loads are $w_{uhpc} = 0.110 \text{ kip/ft}$ and $w_{ws} = 0.058 \text{ kip/ft}$. These values are used in equation 16 by applying appropriate factors to each distributed load and summing the results. The factored distributed dead load, $w_{DL} = 0.168 \text{ kip/ft}$, and $x = 6.667 \text{ inches}$ are substituted into equation 16 and yields the following.

$$M_{C-C:2} = \frac{(4)(0.168 \text{kip/ft})(8 \text{ft})}{10}(0.556 \text{ft}) - \frac{(0.168 \text{kip/ft})(0.556 \text{ft})^2}{2} = \underline{0.273 \text{kipft}}$$

It should be noted the moment caused by the interior dead loads is positive and should be subtracted when adding the negative moments together.

Figure 16 approximates the moment occurring over span 1 due to the collision capacity of the railing. The magnitude of the collision capacity is assumed to be the same at the center line of the exterior girder as at the base of the parapet. The collision capacity at cross section C-C is determined by approximating $M_2/M_1 = 0.4$ and distributing the moment in a similar procedure as in section 3.4.1.2 of this report.

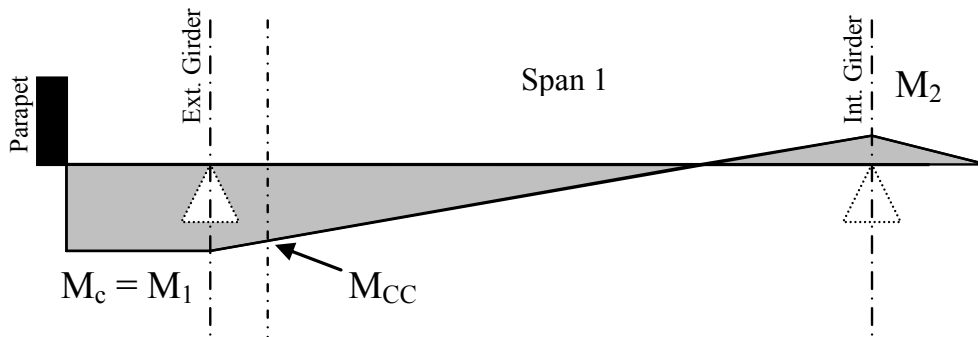


Figure 16. Illustration. Approximate Moment Diagram between Exterior Girder and First Interior Girder Due to Collision Capacity Moment

Collision capacity at section C-C:

$$M_{CC} = 17.83 \text{kipft / ft} \left(1 - \frac{1.4(0.556 \text{ft})}{8 \text{ft}} \right) = 16.095 \text{kipft / ft}$$

Distribution of collision capacity at section C-C over 2 foot width:

$$M_{C-C:coll} = \frac{(16.095 \text{kipft / ft})(19.6 \text{ft})}{19.6 \text{ft} + (2)(1.868 \text{ft})(\tan 30^\circ)} (2 \text{ft}) = \underline{29 \text{kipft}}$$

Factored negative moment at C-C:

$$M_{C-C} = 3.322 \text{kipft} - 0.273 \text{kipft} + 29 \text{kipft} = \underline{\underline{32.049 \text{kipft}}}$$

The transverse collision force at section C-C is determined in the same manner as for section B-B. The tensile force computed in this step is conservative since this method assumes the exterior girder does not provide any lateral restraint against the transverse collision force. Thus, the tensile force at cross section C-C is larger than anticipated and the calculations are as follows.

Tensile collision force at C-C per linear foot:

$$T_{C-C:coll} = \frac{137.22\text{kip}}{19.6\text{ft} + (2)(3.5\text{ft}) + (2)(1.868\text{ft})(\tan 30^\circ)} = 4.772 \frac{\text{kip}}{\text{ft}}$$

Tensile collision force at C-C:

$$T_{C-C} = (2\text{ft}) \left(4.772 \frac{\text{kip}}{\text{ft}} \right) = \underline{\underline{9.54\text{kip}}}$$

For Design Case I at section C-C, the design moment and tensile force are the following:

$$M_{C-C} = \underline{\underline{32.05 \text{ kip ft}}} \quad T_{C-C} = \underline{\underline{9.54 \text{ kip}}}$$

3.4.2 Design Case II: Vertical Collision Force

Design Case II accounts for the vertical forces experienced from a vehicle overtopping on the railing in conjunction with the dead load of the structure. This is categorized as an Extreme Event II limit state and applicable load factors are given in Table 8. This design case generally produces much lower negative moments when compared to Design Case I and III for overhangs with concrete railings. This may not be the case for post and beam railings which would have concentrated loads at the posts. Since a concrete railing is used in this example, Design Case II is not checked since the UHPC deck panel is expected to experience the same loads as a traditional concrete deck.

3.4.3 Design Case III: Dead and Live Loads

Design Case III examines the presence of a live load on the overhang region without a collision force and the self-weight of the structure. This is a Strength I limit state and applicable load factors are given in Table 8. Two sections are considered for this case. These are at the design sections towards the exterior edge of the panel measured from the centerline of the exterior girder and the design section towards the interior of the panel measured from the centerline of the exterior girder. Refer to Figure 9 at sections B-B and C-C for the locations of investigation. For clarity, sections B-B and C-C for Design case III will be referred to as sections D-D and E-E, respectively, to distinguish between the design values for Extreme event II and Strength I limit states.

3.4.3.1 Design Section Towards Exterior of Deck (Section D-D)

A truck wheel load of 16 kips, as suggested by AASHTO LRFD Bridge Design Specifications 3.6.1.2.2, is placed on the overhang region to consider vehicular live load effects. The truck wheel load is modeled by a distributed load acting over a rectangular area with its resultant force located 12 inches from the face of the parapet as specified in AASHTO LRFD Design Specifications 3.6.1.3.1 and illustrated in Figure 17.

Moment at D-D from truck live load:

$$M_{D-D:LL} = \frac{\left(9.60 \frac{\text{kip}}{\text{ft}}\right)(0.59\text{ft})^2}{2} = 1.671\text{kipft}$$

Recalling from Table 8, load factors for Strength I limit state on the overhang region are 1.75 for live load, 1.50 for wearing surface, and 1.25 for dead load components of the structure. In addition to the load factor, the live load must be adjusted with a multiple presence factor, m , and a dynamic load allowance factor, IM , as specified in AASHTO LRFD Bridge Design Specification 3.6.1.1.2 and 3.6.2, respectively. With only one loaded lane possible for section D-D, the multiple presence factor is 1.2. Since the Strength I limit state falls within the “all other limit states” category, the dynamic load allowance is 33% as listed in Table 3.6.2.1-1 of the AASHTO LRFD Bridge Design Specification. The total factored live load moment with appropriate distribution over the equivalent strip and for the 2-foot T-beam cross section is shown below.

Factored live load moment at D-D:

$$M_{D-D:LL} = \frac{(1.75)(1.2)(1.671\text{kipft})(1+33\%)}{4.242\text{ft}}(2\text{ft}) = \underline{2.200\text{kipft}}$$

Referring back to section 3.4.1.2 of this report, the negative unfactored dead load moments used for cross section B-B are the same for cross section D-D. For convenience, negative dead load moments for cross section B-B are listed in Table 9. The appropriate load factors are applied and the factored dead load negative moment is given below.

Table 9. Section B-B and D-D Negative Dead Load Moments

Moment at Section B-B and D-D due to	Value (kip ft)
T-beam	0.276
exterior web	0.082
interior web	0.016
parapet	2.353
wearing surface	0.017

Factored dead load moment at D-D:

$$M_{D-D:DL} = 1.25(0.276\text{kipft} + 0.082\text{kipft} + 0.016\text{kipft} + 2.353\text{kipft}) + 1.50(0.017\text{kipft})$$

$$= \underline{3.434\text{kipft}}$$

Factored negative moment at D-D

$$M_{D-D} = 2.200\text{kipft} + 3.434\text{kipft} = \underline{\underline{5.634\text{kipft}}}$$

For Strength I limit state at cross section D-D, the negative moment of 5.634 kip-ft is considerably less when compared to the Extreme Event II limit state at the same section.

3.4.3.2 Design Section Towards Interior of Deck (Section E-E)

For cross section E-E, a truck axle with a total weight of 32 kips is placed on the deck such that one 16 kip wheel load is 1 foot away from the parapet face and the other 16 kip wheel load is spaced 6 feet away from the companion wheel load as specified in AASHTO LRFD Bridge Design Specification 3.6.1.2.2. The bending moment at cross section E-E is modeled by applying two wheel point loads on a simply supported beam with supports at the exterior girder and the first interior girder spaced at 8 feet. Figure 18 shows the location of the wheel loads with respect to the parapet and concrete girders. Performing an equilibrium analysis gives the following reaction at the exterior girder from the live loads.

$$\sum M_{right\ support} = (16\text{kip})(27.75\text{in}) + (16\text{kip})(99.75\text{in}) - R_{ext\ gir} (96\text{in})$$

$$\therefore R_{ext\ gir} = 21.25\text{kip}$$

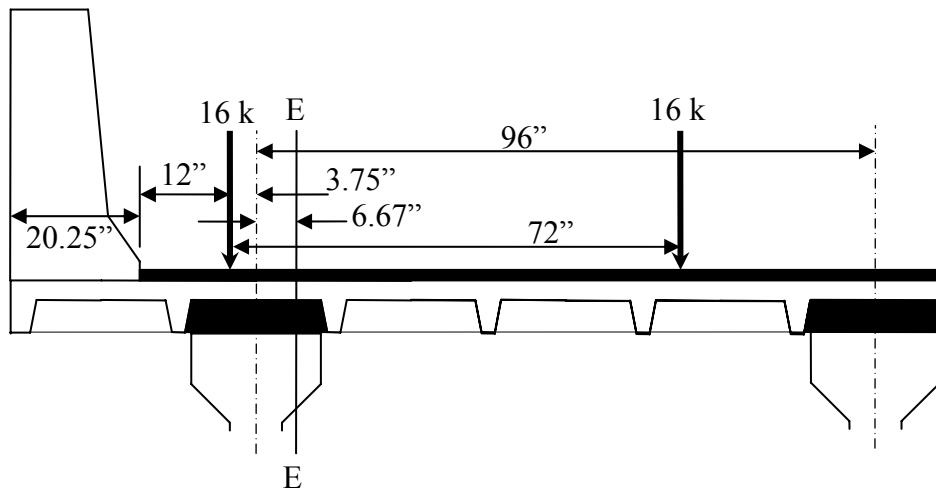


Figure 18. Illustration. Section E-E of the Overhang

The live load moment is then determined by examining cross section E-E and ensuring that equilibrium is satisfied by using the exterior girder reaction computed in the previous step. The sketch of the free body diagram of the exterior girder is shown in Figure 19 with the accompanying moment equation following.

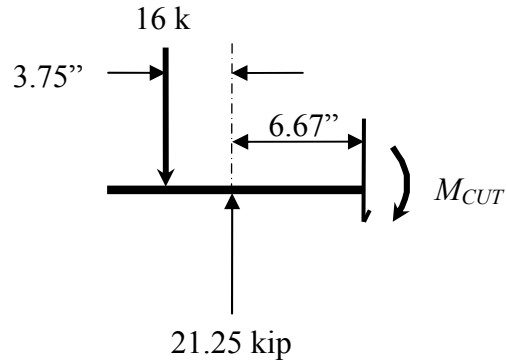


Figure 19. Illustration. Free Body Diagram for Section E-E

$$\sum M_{cut} = (16\text{kip})(10.42\text{in}) - (21.25\text{kip})(6.67\text{in}) - M_{CUT}$$

$$\therefore M_{CUT} = 24.9825\text{kipin} = 2.082\text{kipft}$$

The live load negative moment from the truck load at cross section E-E is 2.082 kip-ft. The maximum negative moment at E-E is generated by placing the concentrated wheel load 1 foot from the face of the parapet. The 1 foot distance between the truck load and the parapet must be maintained as specified by AASTHO LRFD Bridge Design Specification 3.6.1.3.1. Moving the truck axle to the right and away from the parapet face would actually decrease the magnitude of the negative moment. As with the live load on section D-D, the wheel loads may be distributed over an equivalent design strip. Since wheel loads on the overhang produce the negative moment, the equivalent strip designated for an overhang is used as specified in AASHTO LRFD Bridge Design Specification 4.6.2.1.3 and determined by equation (17). The distance between the point load to the exterior girder support for this loading state is $X = 3.75$ inches. Thus the equivalent strip for cross section E-E is shown in the following step.

Equivalent strip for section E-E:

$$w_{strip:E-E} = 45.0\text{in} + 10.0\text{in} \frac{0.3125\text{ft}}{\text{ft}} = 48.125\text{in} = 4.010\text{ft}$$

Given the load, presence, and dynamic allowance factors established in section 3.4.3.1 of this report, the negative live load moment at E-E for a 2 foot wide cross section is shown in the following step.

Factored live load moment at E-E:

$$M_{E-E:LL} = \frac{(1.75)(1.2)(2.082\text{kipft})(1 + 33\%)}{4.010\text{ft}} (2\text{ft}) = \underline{2.900\text{kipft}}$$

The unfactored negative dead load moments acting at E-E are similar to the loads on C-C. The negative dead load moments on cross section E-E are factored for the Strength I limit state. These load factors are presented in Table 8 of this report. Recall that the computed dead load

moment calculations for cross section C-C were performed in separate steps and then the results were superimposed. The two components contributing to the negative moment are from the dead loads on the overhang region and the interior bays. Moments at cross section C-C caused by overhang loads are listed in Table 10 for convenience to the reader. A similar analysis procedure as detailed in section 3.4.1.3 of this report is followed to determine the factored negative dead load moment at cross section E-E.

Table 10. Section C-C and E-E Negative Dead Load Moments

Moment at Section C-C and E-E due to	Value (kip ft)
T-beam	0.416
exterior web	0.102
interior web	0.036
Parapet	3.076
wearing surface	0.050

Factored negative moment at centerline of exterior girder due to dead loads on the overhang:

$$M_{GU} = 1.25(0.416\text{kipft} + 0.102\text{kipft} + 0.036\text{kipft} + 3.076\text{kipft}) + 1.50(0.050\text{kipft}) = 4.60125\text{kipft}$$

Referring to Figure 14, the negative moment due to loads on the overhang is determined by using similar triangles and establishing $M_2/M_1 = 0.4$.

Factored negative moment at section E-E due to dead loads on the overhang:

$$M_{E-E:1} = 4.60125\text{kipft} \left(1 - \frac{1.4(0.556\text{ft})}{8\text{ft}} \right) = \underline{4.164\text{kipft}}$$

Figure 15 and equation (16) are referenced to determine the moment at E-E from the dead loads on the interior bays. Distributed dead loads for the UHPC deck and wearing surface are $w_{uhpc} = 0.110 \text{ kip/ft}$ and $w_{ws} = 0.058 \text{ kip/ft}$. Recall that these dead loads cause positive bending and thus must be subtracted from the negative moment caused by the overhang loads.

Factored uniform dead load on interior bays:

$$w_{DU} = 1.25(0.110 \text{ kip/ft}) + 1.5(0.058 \text{ kip/ft}) = 0.2245 \text{ kip/ft}$$

Substituting the factored uniform dead load into equation (16) gives the following positive moment at cross section E-E.

$$M_{E-E:2} = \frac{(4)(0.2245\text{kip/ft})(8\text{ft})}{10}(0.556\text{ft}) - \frac{(0.2245\text{kip/ft})(0.556\text{ft})^2}{2} = \underline{0.365\text{kipft}}$$

The factored live load moment and the two factored dead load moments are combined for the resulting factored negative moment at E-E in the following step.

Factored negative moment at E-E:

$$M_{E-E} = 2.900\text{kipft} + 4.164\text{kipft} - 0.365\text{kipft} = \underline{\underline{6.699\text{kipft}}}$$

For Design Case III at section E-E, the design moment is the following:

$$M_{E-E} = \underline{\underline{6.699 \text{ kip ft}}}$$

3.5 SUMMARY OF DESIGN LOADS

For the given UHPC bridge deck cross section, parapet, and bridge deck system geometry, a summary of the expected design loads is given in this section. The positive and negative live load moments for the UHPC deck element at interior bays and over interior girders were determined by a simplified procedure as described in AASHTO LRFD Bridge Design Specification Appendix A4. The values given by this approach are generally conservative for both negative and positive bending within the interior region of the deck. The interior region moments are listed in Table 11.

Table 11. Design Moments for Interior Deck Region

Location	Value (kip-ft)
interior bays (positive bending)	21.36
over interior girder (negative bending)	18.28

The overhang region is typically checked for three different cases at several locations around the overhang region. For this example, only design case I and III were examined since design case II seldom gives the limiting moments. Refer to Figure 9 and section 3.4 of this report for detailed descriptions of the design cases and sections for examination. The moments and axial tensile forces, if applicable, are listed in Table 12 for the different design cases and locations which were examined.

Table 12. Design Negative Moments for Overhang Region

Design Case	Section	Moment (kip-ft)	Tensile Force (kip)
I	A-A	37.22	10.32
I	B-B	36.88	9.99
I	C-C	32.05	9.54
III	D-D	5.63	N/A
III	E-E	6.70	N/A

Given the established positive and negative moments for the interior bays (Table 7) and negative moments for the overhang region with accompanying tensile forces (Table 8), the next step is to determine the moment capacity of the cross section in both positive and negative bending. The next chapter details the moment capacity analysis procedure of the two-way ribbed deck slab.

CHAPTER 4. FLEXURAL CAPACITY ANALYSIS OF UHPC DECK SLAB

The positive and negative transverse moment capacity for the proposed cross section is determined by applying the methodology detailed in Chapter 2 and using the properties and characteristics of the cross section. For convenience, the T-beam cross section, beam dimensions, and cross sectional properties are reproduced here for the reader in Figure 20, Table 13, and Table 14, respectively.

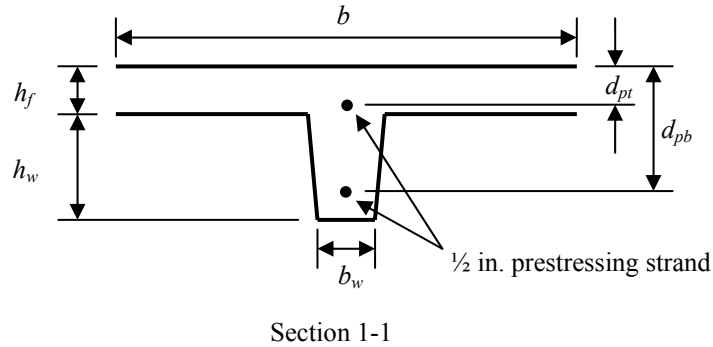


Figure 20. Illustration. UHPC Transverse Strip Cross Section

Table 13. T-Beam Dimensions

Property	Dimension
Effective width, b	24 in.
Flange thickness, h_f	2 ½ in.
Web height, h_w	5 ½ in.
Web width, b_w	3 in.
Top strand depth, d_{pt}	2 in.
Bottom strand depth, d_{pb}	6 ½ in.

Table 14. T-Beam Properties

Property	Dimension
Cross sectional area, A_c	76.5 in. ²
Centroid axis– measured from bottom, y_c	5.89 in.
Moment of inertia, I_c	279.9 in. ⁴
Radius of gyration, r	1.913 in.
Strand area, A_p	0.153 in. ²
Top strand eccentricity, e_t	-0.1127 in.
Bottom strand eccentricity, e_b	4.3873 in.

4.1 PARAMETERS AND ASSUMPTIONS

The UHPC deck element is precast and prestressed with two ½ inch diameter low relaxation 270 ksi strands along the centerline of the transverse web as shown in Figure 20. The strands are pretensioned in such a manner which allows the effective prestress to be 140.5 ksi after prestress losses. Relevant parameters for the UHPC flexural behavior model and prestressing strands are presented in Table 15.

Table 15. Deck Panel Material Properties

Property	Value
UHPC modulus of elasticity, E	7600 ksi
UHPC limiting compressive strength, f_{mc}	23.8 ksi
UHPC sustainable tensile strength, f_{mt}	1.125 ksi
UHPC limiting compressive strain, ε_{mc}	0.003132
UHPC limiting tensile strain, ε_{mt}	0.007
prestressing strand ultimate tensile strength, f_{pu}	270 ksi
prestressing strand modulus of elasticity, E_p	28500 ksi

The assumed stress-strain curve for a 270 ksi low-relaxation prestressing strand is shown in Figure 21. The stress-strain relationship is expressed by equation (18).⁽⁷⁾

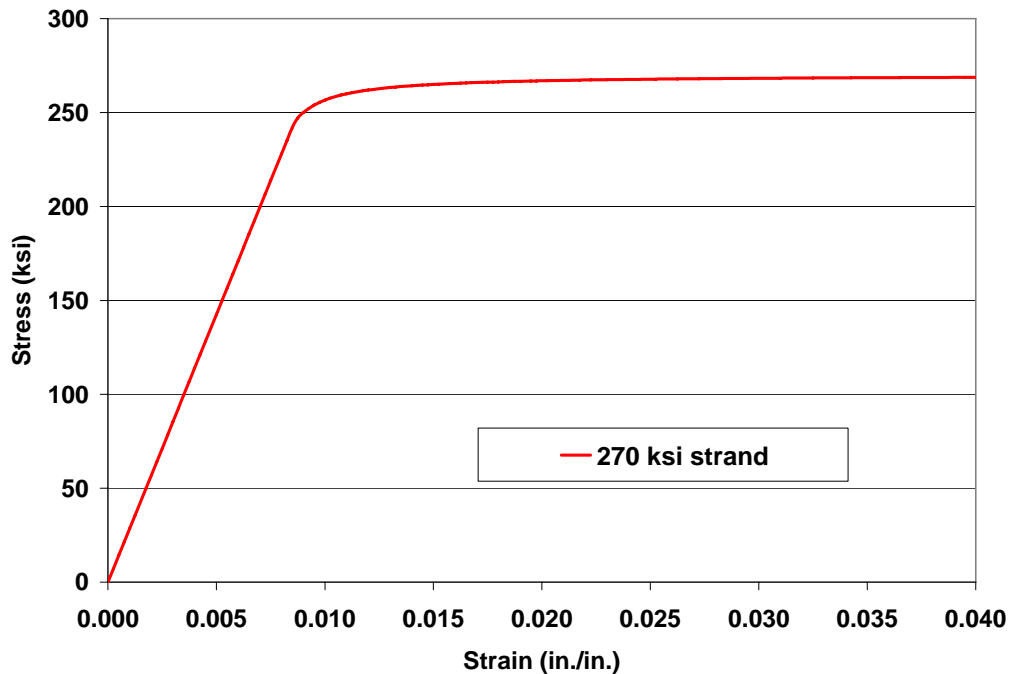


Figure 21. Graph. Prestressing Strand Stress Strain Model

Stress in 270 ksi strand:

$$\begin{aligned}
 f_{ps,270} &= E_p \varepsilon_{ps} \quad \text{if } \varepsilon_{ps} \leq 0.0086 \\
 &= 270\text{ksi} - \frac{0.04\text{ksi}}{\varepsilon_{ps} - 0.007} \quad \text{if } \varepsilon_{ps} > 0.0086
 \end{aligned}
 \tag{18}$$

4.2 POSITIVE BENDING MOMENT CAPACITY

The procedure outlined in the flowchart of Figure 6 will be followed to determine the positive and negative moments for the T-beam cross section. The dimensions and properties for the cross section have been established in Tables 13 and 14. Additionally, the limiting tensile and compressive strains and stresses are listed in Table 15. Next, the effective prestress, ε_{pe} , and decompression strain, ε_2 , are determined by equations (19) and (20).

$$\varepsilon_{pe} = \frac{P_e}{A_p E_p} \tag{19}$$

$$\varepsilon_2 = \frac{1}{A_c E_c} \left(P_e + \frac{M_p e}{r^2} \right) \tag{20}$$

For equations (19) and (20), P_e/A_p is the effective prestress, P_e is the total force exerted on the cross section from the strands, A_p is the area of the prestressing strand, A_c is the area of the UHPC cross section, M_p is the moment produced from the strands, e is the eccentricity of the strands, and r is the radius of gyration for the UHPC cross section. For this example, each of the two strands is assumed to have the same effective prestress. The corresponding strain for each strand is shown below.

$$\varepsilon_{pe} = \frac{140.5\text{ksi}}{28500\text{ksi}} = 0.004931$$

Before determining decompression strain, the internal moment produced from the eccentric forces of the prestressing strands are calculated. Given the effective stress and the area of the strands, the effective force in each strand is 21.5 kip. The resulting internal negative moment from the strands, as shown in Figure 22, is the shown in the following calculation.

$$M_p = (21.5\text{kip})(4.387\text{in}) - (21.5\text{kip})(0.113\text{in}) = 91.90\text{kipin} = 7.658\text{kipft}$$

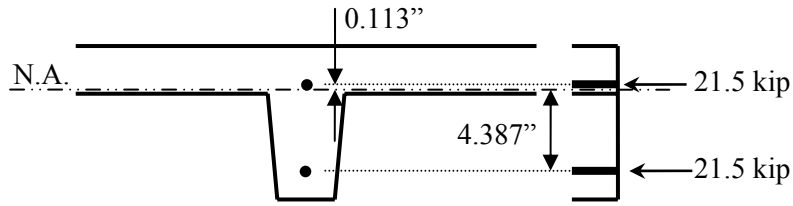


Figure 22. Illustration. Strand Location and Force on Cross Section

The decompression strain for locations of the top and bottom strands are calculated below.

Top strand decompression:

$$\epsilon_{2t} = \frac{1}{(76.5\text{in}^2)(7600\text{ksi})} \left(43\text{kip} + \frac{(7.658\text{kipft}) \frac{12\text{in}}{\text{ft}} (-0.113\text{in})}{(1.913\text{in})^2} \right) = 0.000069$$

Bottom strand decompression:

$$\epsilon_{2b} = \frac{1}{(76.5\text{in}^2)(7600\text{ksi})} \left(43\text{kip} + \frac{(7.658\text{kipft}) \frac{12\text{in}}{\text{ft}} (4.387\text{in})}{(1.913\text{in})^2} \right) = 0.000264$$

Before the deck element is loaded, the cross section is in the state of strain shown in Figure 23. The cross section is in compression at the bottom and experiences slight tension in the uppermost top flange. The origin of zero strain for the strands has been offset to illustrate the amount of effective prestress strain in the strands before decompression occurs. When the T-beam is loaded in positive bending, the cross section undergoes decompression to a state of zero strain. The decompression of the UHPC around the prestressing strands is the portion of the strain line corresponding to the strand which is within the shaded area in Figure 23. The final state of the cross section will be shown once the neutral axis is determined which causes the maximum moment capacity.

As a guide for establishing the type of failure for the UHPC cross section, the positive bending balanced failure neutral axis depth, c_{b+} , is calculated using equation 10. Referring to Figure 6, if the initial guess for the neutral axis is less than c_{b+} , the cross section has reached the defined limiting tensile strain of the UHPC. If c is greater than c_{b+} , the cross section is at the limiting UHPC compressive strength stipulated by the flexural behavior model. The neutral axis depth for a positive bending balanced failure is shown in the next step.

$$c_{b+} = \frac{0.003132}{0.003132 + 0.007} (8\text{in}) = 2.47\text{in}$$

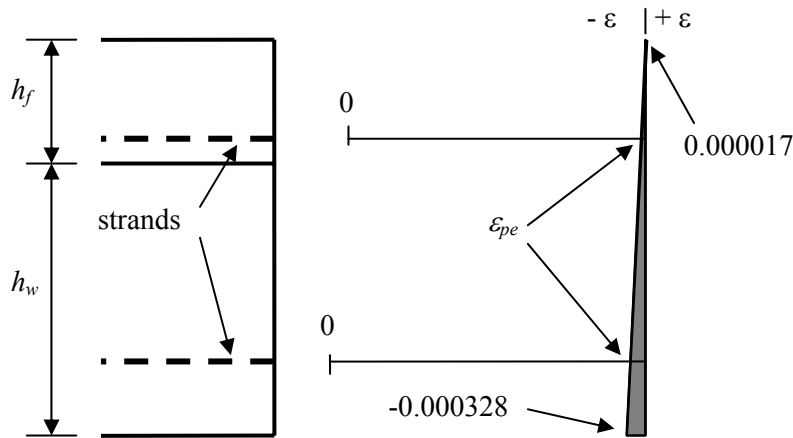


Figure 23. Illustration. Cross Section Strain before Positive Bending

Through a series of iterations, the neutral axis depth for the T-beam cross section in positive bending is determined to be 1.138 inches. The neutral axis depth is less than c_{b+} and therefore the maximum moment capacity for the cross section is limited by the tensile constraints of the UHPC model. Limiting tensile values for the cross section therefore are $\epsilon_{mt} = 0.007$ and $f_{mt} = 1.125$ ksi. The compressive strain at the top of the cross section is calculated to establish the appropriate compressive stress in the compression zone.

$$\epsilon_c = \frac{1.138\text{in}}{8\text{in} - 1.138\text{in}}(0.007) = 0.001161$$

The compressive strain at the top of the section is within the limiting strain of 0.003132 for the UHPC. Since the compressive strain does not reach its limit, only a portion of the compressive strength is developed. Referring back to Figure 6, the compressive stress at this state of strain can be determined with the following calculation.

$$f_c = 7600\text{ksi}(0.001161) = 8.82\text{ksi}$$

The following calculations show the additional strain required in each strand to attain equilibrium and moment capacity of the cross section.

Required strain to develop moment capacity for top and bottom strands:

$$\epsilon_{3t} = \frac{2\text{in} - 1.138\text{in}}{8\text{in} - 1.138\text{in}}(0.007) = 0.000879$$

$$\epsilon_{3b} = \frac{6.5\text{in} - 1.138\text{in}}{8\text{in} - 1.138\text{in}}(0.007) = 0.005470$$

Strain portions for each strand are summed together for the total strain experienced in each of the strands.

Total strain for top and bottom strands:

$$\epsilon_{pst} = 0.004931 + 0.00006909 + 0.000879 = 0.005879$$

$$\epsilon_{psb} = 0.004931 + 0.0002635 + 0.005470 = 0.010665$$

The state of strain for the UHPC cross section at nominal positive moment capacity is shown in Figure 24.

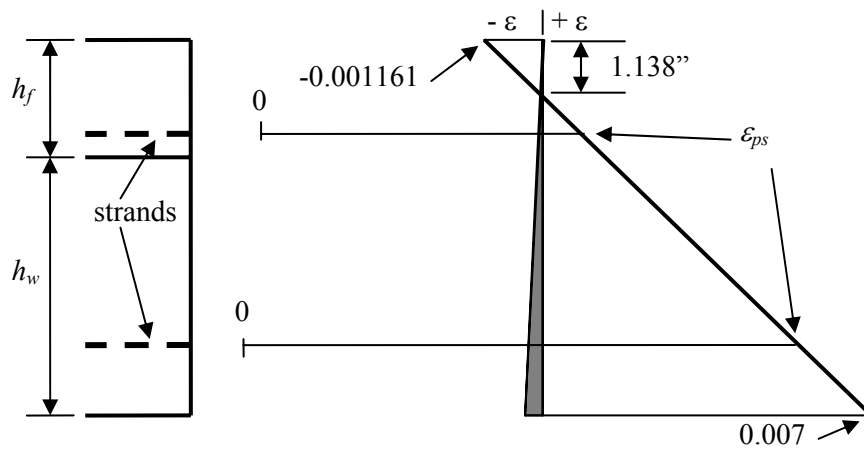


Figure 24. Illustration. Strain at Moment Capacity for Positive Bending

Resulting strain calculations indicate the top strand to be within the linear portion of the stress strain curve while the bottom strand is starting to yield. Equation (18) is used for the stresses in the strand.

Tensile stress for top and bottom strands:

$$f_{sst} = 28500\text{ksi}(0.005879) = 167.55\text{ksi}$$

$$f_{ssb} = 270\text{ksi} - \frac{0.04\text{ksi}}{0.010665 - 0.007} = 259.09\text{ksi}$$

With stresses known for the UHPC in tension and compression and the tensile stresses in each of the strands, the internal forces in the member can be computed. Figure 25 shows the stress distributions within the cross section which are then used to determine the forces and the moment capacity of the beam.

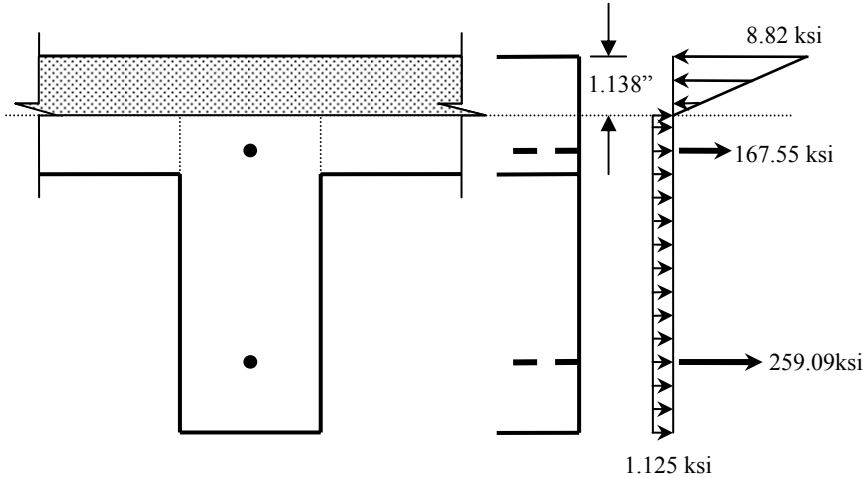


Figure 25. Illustration. Cross Section Stress Distribution for Positive Bending

The next step is to determine the tensile force for each strand by using equation 2. The area of each strand is 0.153in.^2 , thus the corresponding forces are,

$$T_{pst} = 167.55\text{ksi}(0.153\text{in}^2) = \underline{25.64\text{kip}}$$

$$T_{psb} = 259.09\text{ksi}(0.153\text{in}^2) = \underline{39.64\text{kip}}$$

Since the neutral axis extends 1.138 inches below the top surface, only a portion of the flange is in compression as shown by the shaded area in Figure 25. Recall from Chapter 2, the compressive stress of UHPC is modeled by a triangular distributed load and, for the current problem and state of strain, the corresponding compressive stress reaches 8.82 ksi. The compressive force in positive bending is the following.

$$C = \frac{1}{2}(8.82\text{ksi})(1.138\text{in})(24\text{in}) = \underline{120.45\text{kip}}$$

From the geometry of the cross section, it is observed that the tension zone includes the web and a portion of the flange. To facilitate moment capacity analysis, the tension zone is broken up into two parts. One part includes the entire width of the web extending from the bottom of the web up to the neutral axis. The other part is taken as having a height equal to flange height in tension with a width equal to the width of the flange minus the web width. These are slight changes to equation (9) but still apply the same basic principle described in Chapter 2.

Tension in UHPC web:

$$T_{cw} = (1.125\text{ksi})(8\text{in} - 1.138\text{in})(3\text{in}) = \underline{23.16\text{kip}}$$

Tension in UHPC flange:

$$T_{cf} = (1.125\text{ksi})(2.5\text{in} - 1.138\text{in})(24\text{in} - 3\text{in}) = \underline{32.18\text{kip}}$$

Knowing all the force components acting within the cross section, a check is performed to verify the internal forces are in equilibrium. Compressive forces should approximately equal the tensile forces as shown in the next step.

$$120.45\text{kip} \cong (25.64 + 39.64 + 23.16 + 32.18)\text{kip} = 120.62\text{kip}$$

As observed from the previous calculation, an acceptable error in equilibrium is achieved and thus further iterations and a new guess at the neutral axis are not required. Had an acceptable level of equilibrium not been achieved, a new guess for c would be required and the process would have to be repeated as detailed in Figure 6.

The number of iterations required to achieve an acceptable level of equilibrium depends on the procedure used to guess a new value of c . A revised form of equation 12 which accounts for a T-beam geometry can be used as a guide for a new c value. However, strictly using the value of c from the revised form of equation 12 for subsequent iterations may diverge from a solution. A good practice is to utilize the average between the previous guess of c and one computed from the revised form of equation 12 as the new guess for the next iteration. After some experience with several iterations and design examples, the designer may get a feel for the sensitivity of the analysis.

With the section in equilibrium, the moment capacity is determined by taking moments about a point on the cross section. This example sums moments about a point on the top surface of the cross section. Figure 26 shows the internal forces on the cross section with applicable dimensions.

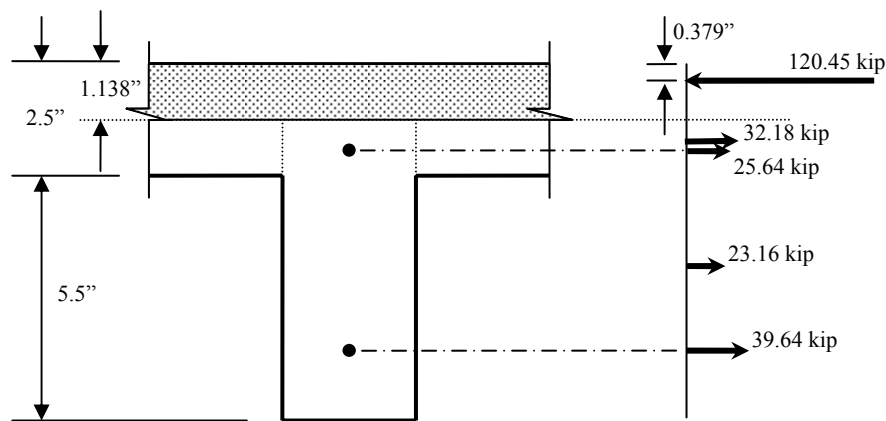


Figure 26. Illustration. Cross Section Forces for Positive Bending

UHPC moment capacity in positive bending:

$$M_{n+} = -120.45\text{kip}\left(\frac{1.138\text{in}}{3}\right) + 32.18\text{kip}\left(\frac{2.5\text{in} + 1.138\text{in}}{2}\right) + 25.64\text{kip}(2\text{in}) \\ + 23.16\text{kip}\left(\frac{8\text{in} + 1.138\text{in}}{2}\right) + 39.64\text{kip}(6.5\text{in}) = 427.60\text{kipin} = \underline{\underline{35.63\text{kipft}}}$$

For the given dimensions, material properties, and UHPC material response methodology, the nominal positive moment capacity for the UHPC T-beam cross section is 35.63 kip-ft. A resistance factor is not applied to the nominal moment since limited statistical data is available on UHPC material variance, workmanship, or quality control. AASHTO LRFD Bridge Design Specifications Section 5.5.4.2 requires a resistance factor of 1.0 for tension-controlled prestressed concrete sections and the UHPC concrete section would fall closest to this category if a factor had to be applied to the nominal moment capacity. Comparing the nominal capacity of the cross section with the design moment of 21.36 kip-ft, reveals the cross section is adequate in resisting positive bending.

4.3 NEGATIVE BENDING MOMENT CAPACITY

A similar procedure as described in section 4.2 of this report is followed to analyze the negative moment capacity of the cross section. Since the same effective prestress in the strands are assumed throughout the length of the T-beam, initial states of strain within the cross section prior to negative bending are the same as they were for the positive bending case. Strains for the strands and UHPC prior to negative bending are shown in Figure 27.

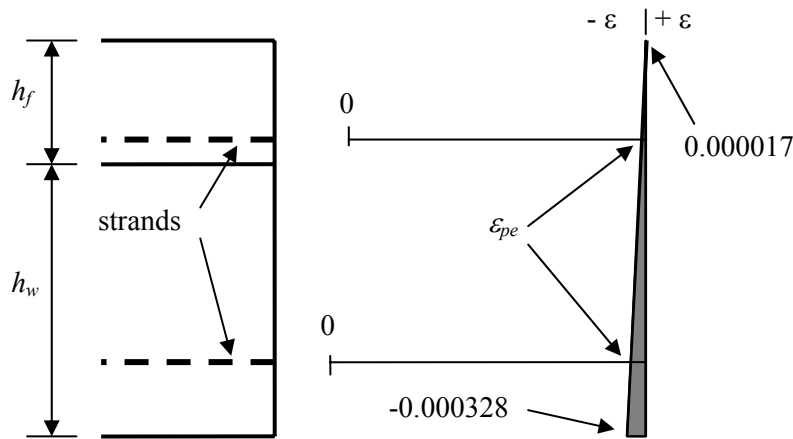


Figure 27 Illustration. Cross Section Strain before Negative Bending

The effective prestress and decompression strains are the following:

$$\varepsilon_{pe} = 0.004931 \quad \varepsilon_{2t} = 0.000069 \quad \varepsilon_{2b} = 0.000264$$

When the member undergoes negative bending, the bottom UHPC section does not decompress as in positive bending, but rather goes into further compression. The eccentricity and prestress of the strands induce initial negative bending and thus subtract from the total potential negative moment capacity.

With geometric dimensions, material properties, ϵ_{pe} , and ϵ_{p2} established, the next step in the analysis flowchart is to determine c_b . This value is computed by equation 11 since the analysis is for negative bending. With negative bending, the top fiber of the member is in tension while bottom fiber is in compression. The balanced failure neutral axis depth for negative bending is shown in the next step.

$$c_b = \frac{0.007}{0.003132 + 0.007}(8\text{in}) = 5.53\text{in.}$$

Since the member is in negative bending, any initial guess of c is checked with the negative Boolean inequality to properly proceed along the flowchart in Figure 6. After a number of iterations, it is determined that the neutral axis for negative bending is $c = 4.59$ inches. This value for neutral axis is less than the balanced failure neutral axis depth and therefore the analysis procedure proceeds to the right of the flowchart. Thus the section is designed to carry load until the limiting compressive stress at the bottom of the UHPC T-beam is reached.

Since compression of the UHPC is the limiting design parameter, values for maximum allowable compressive strain, maximum allowable compressive stress, and maximum usable tensile stress for design are 0.003132, 23.8 ksi, and 1.125 ksi, respectfully. Tensile strain in the top fibers of the UHPC is shown in the following calculation.

$$\epsilon_t = \frac{4.59\text{in}}{8\text{in} - 4.59\text{in}}(0.003132) = 0.004213$$

The strains in each strand required to achieve equilibrium for the cross section in negative bending are the following.

$$\epsilon_{3t} = \frac{2\text{in} - 4.59\text{in}}{8\text{in} - 4.59\text{in}}(-0.003132) = 0.002379$$

$$\epsilon_{3b} = \frac{6.5\text{in} - 4.59\text{in}}{8\text{in} - 4.59\text{in}}(-0.003132) = -0.001754$$

The strain for the bottom strand location, ϵ_{3b} , to achieve equilibrium is negative and thus reveals the UHPC around the bottom strand is in compression while the UHPC around the top strand is in tension. By algebraically summing the three different components of strain for the strands, the total strain and tensile stress can be computed.

Total strain for top and bottom strands:

$$\epsilon_{pst} = 0.004931 + 0.00006909 + 0.002379 = 0.007379$$

$$\epsilon_{psb} = 0.004931 + 0.0002635 - 0.001754 = 0.003441$$

The state of strain for the cross section at nominal negative moment capacity is shown in Figure 28.

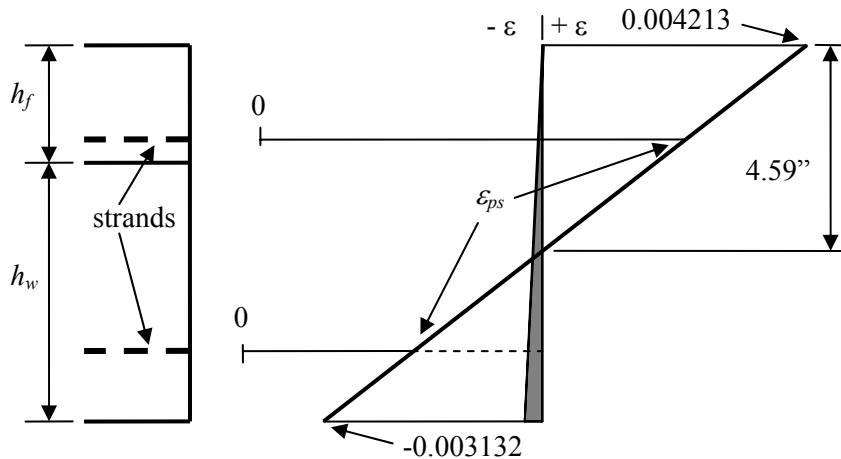


Figure 28. Illustration. Strain at Moment Capacity for Negative Bending

The total strain for each strand is below 0.0086 and therefore within the linear elastic region of the stress strain curve in Figure 21 and the accompanying strand stresses are computed with equation (18) and shown below.

Tensile stress for top and bottom strands:

$$f_{sst} = 28500\text{ksi}(0.007379) = 210.30\text{ksi}$$

$$f_{ssb} = 28500\text{ksi}(0.003441) = 98.07\text{ksi}$$

Figure 29 illustrates the stress distributions for the different components within the cross section which are used to determine the forces and subsequent negative moment capacity of the beam.

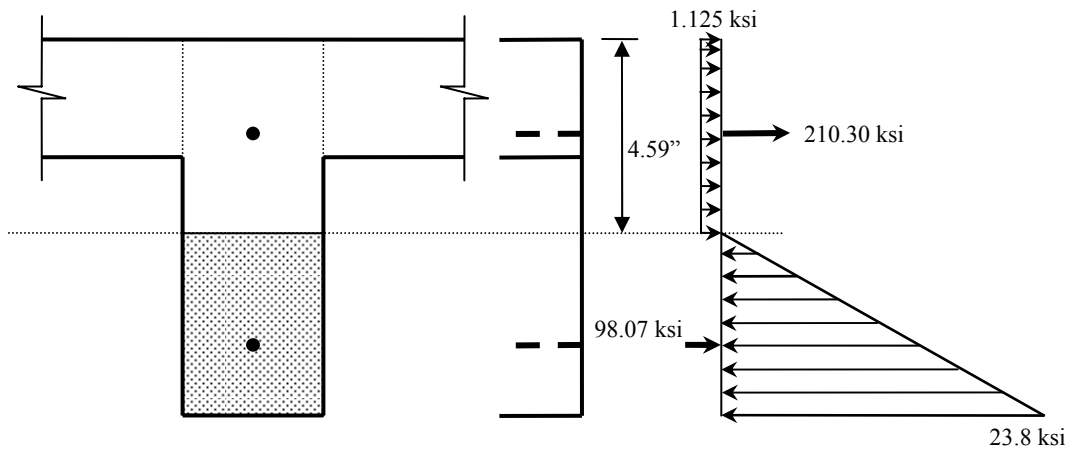


Figure 29. Illustration. Cross Section Stress Distribution for Negative Bending

Similar concepts used in section 4.2 are used to determine the tensile forces in the strands and UHPC, and compressive force in the UHPC.

Tensile force in strands:

$$T_{pst} = 210.30\text{ksi}(0.153\text{in}^2) = \underline{32.18\text{kip}}$$

$$T_{psb} = 98.07\text{ksi}(0.153\text{in}^2) = \underline{15.00\text{kip}}$$

Tension in UHPC web:

$$T_{cw} = (1.125\text{ksi})(4.59\text{in})(3\text{in}) = \underline{15.49\text{kip}}$$

Tension in UHPC flange:

$$T_{cf} = (1.125\text{ksi})(2.5\text{in})(24\text{in} - 3\text{in}) = \underline{59.06\text{kip}}$$

Compression in UHPC flange:

$$C = \frac{1}{2}(23.8\text{ksi})(8\text{in} - 4.59\text{in})(3\text{in}) = \underline{121.74\text{kip}}$$

Internal forces are summed to check for equilibrium:

$$121.74\text{kip} \cong (32.18 + 15.00 + 15.49 + 59.06)\text{kip} = 121.73\text{kip}$$

With an acceptable state of equilibrium, the nominal negative moment for the cross section is computed. Figure 30 shows the resultant forces acting on the cross section. Moments are taken from the top of the section.

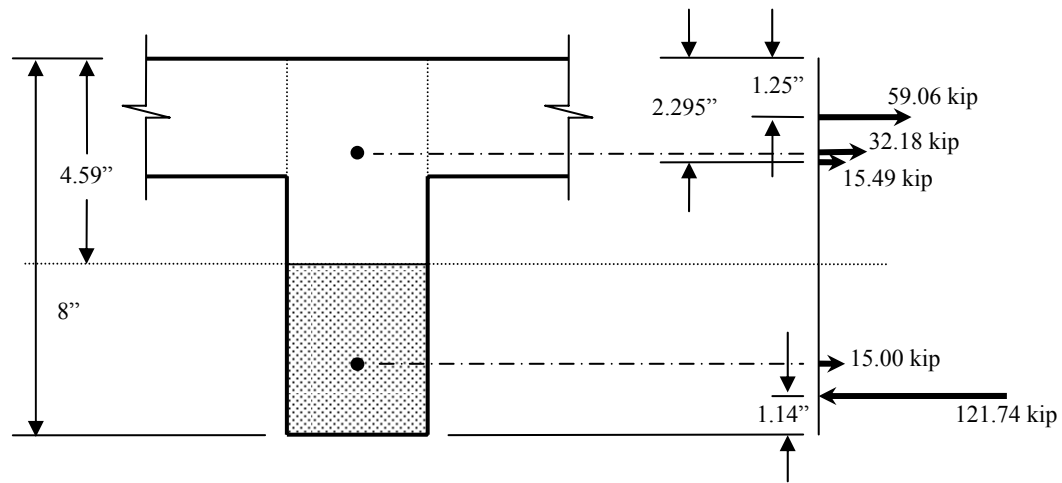


Figure 30. Illustration. Cross Section Forces for Negative Bending

UHPC moment capacity in negative bending:

$$\begin{aligned}
 M_{n-} &= 59.06\text{kip}(1.25\text{in}) + 32.18\text{kip}(2\text{in}) + 15.49\text{kip}\left(\frac{4.59\text{in}}{2}\right) \\
 &+ 15.00\text{kip}(6.5\text{in}) - 121.74\text{kip}\left(\frac{2(8\text{in}) + 4.59\text{in}}{3}\right) = -564.3\text{kipin} = \underline{\underline{-47.03\text{kipft}}}
 \end{aligned}$$

In negative bending, the UHPC T-beam has a capacity of 47.03 kip-ft. Comparing this value to the design negative moment of 18.28 kip-ft over girders in the interior region, the T-beam is adequate in providing the necessary resistance. The negative moment however must be compared to the negative design moments from the overhang region. The overhang region experiences both negative bending and an axial tensile force for the Extreme Event II limit state. To verify if the cross section can withstand the combination of both bending and axial design loads, an interaction curve is developed for the T-beam. The interaction curve conceptually states that the UHPC cross section has maximum negative moment capacity when no axial force occurs and similarly, the cross section has maximum axial tensile resistance without the presence of bending.

Through the analysis for negative moment capacity, it is established that the T-beam resists a negative moment of 47.03 kip-ft without the presence of an axial load on the cross section. To determine the negative moment capacity of the T-beam over a range of axial loads, the cross section is analyzed by superimposing increasing increments of tensile strain to the strain profile corresponding to the negative moment capacity. Each analysis of superimposed strains yields a negative moment and axial load the cross section is able to resist. This analysis is performed

until the cross section reaches the permissible tensile strain, ϵ_{mt} , of 0.007. Figure 31 illustrates the superposition of the strain profiles used to determine pairs of moments and axial loads.

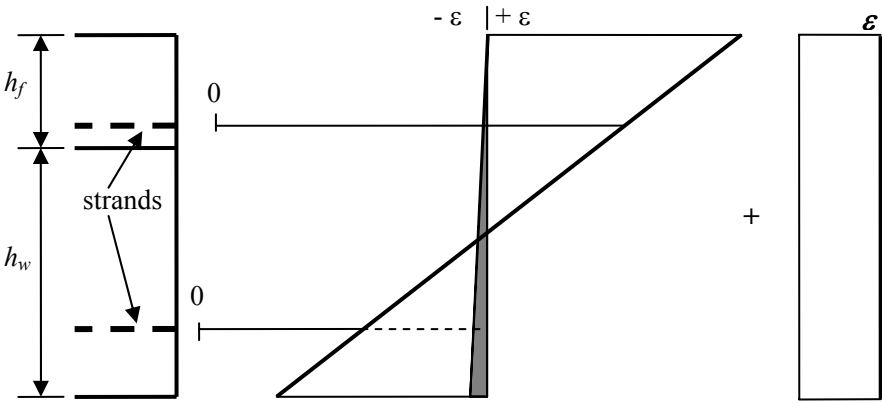


Figure 31. Illustration. Strain Superposition for Interaction Curve

The strain analysis of the T-beam indicates that a maximum axial load of 124 kip can be resisted when no bending moment is applied. Several other moment and axial load combinations are determined to get a defined interaction curve. The interaction curve shows the boundary of the negative moment and axial load combinations. For the given cross section in this report, any moment and axial load combination below the interaction curve would be within the capacity of the T-beam. For example, a T-beam with the same geometric, material, and behavioral properties as in this report would be within the limits of sustaining a negative moment of 30 kip-ft with an approximate 50 kip tensile axial load. Figure 32 presents the interaction curve for the given T-beam cross section.

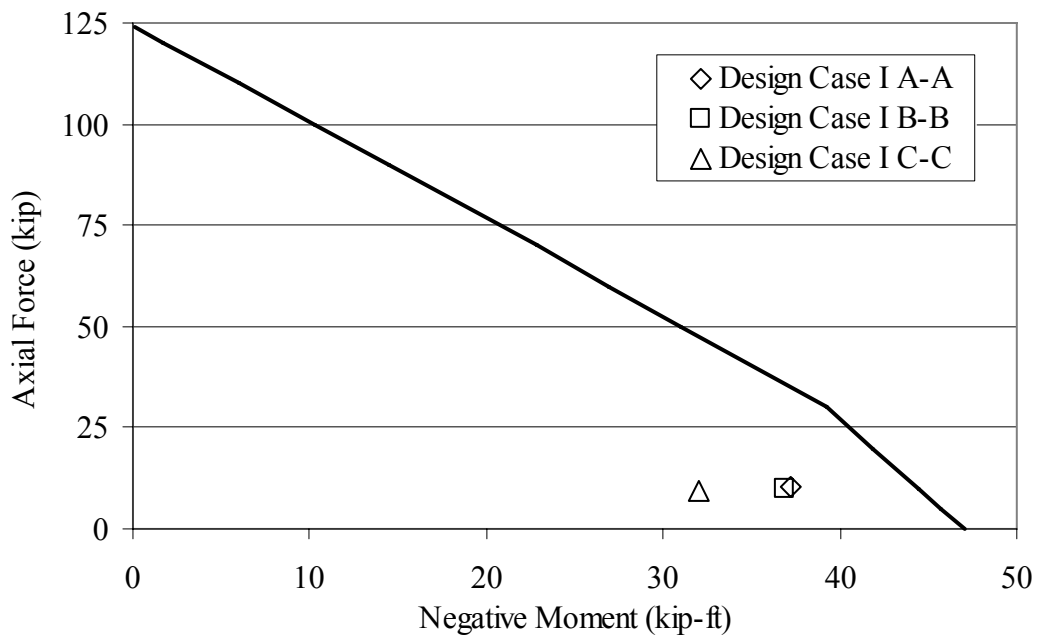


Figure 32. Graph. Interaction Curve for Negative Bending and Axial Tension

Along with the interaction curve in Figure 32, the negative design moment and axial design load combinations from Design Case I of the overhang have been included in the graph. The three design combinations, as listed in Table 12, appear on the lower right portion of the graph between 30 and 40 kip-ft. Since the three design combinations are below the interaction curve boundary, the T-beam is able to resist the design load combinations of the overhang.

CHAPTER 5. OVERVIEW OF DESIGN LOADS AND MOMENT CAPACITY

The design example presented in this report made several assumptions about the behavior of the bridge deck system and its analysis. It was assumed that:

- adequate anchorage between UHPC deck panel and girders is provided,
- adequate anchorage between concrete railing and deck panel exists,
- a connection system is effective in transmitting loads between adjacent deck panels,
- moments and axial forces distribute outward at 30° as typically assumed in concrete design,
- the effective flange width for concrete as specified in AASHTO LRFD Bridge Design Specifications can be used for UHPC,
- the entire effective flange width may take uniform tension when considering negative bending,
- the design section for negative moment analysis as specified in the AASHTO LRFD Bridge Design Specifications can be used for UHPC,
- the UHPC allowable design tensile stress is 1.125 ksi for tensile strains between 0.000 and 0.007, and
- an interaction curve can be used to assess the resistance of a moment and axial force combination.

This report used portions of the AASHTO specifications and results of previous UHPC studies to determine design loads and moment capacities for a prestressed UHPC member. This example serves only as a guideline and accepted specifications for UHPC design must be developed. In addition, the effective prestress in the strands for this example was an assumed value based on limited research.

A recap of the design moments and axial forces reveal the cross section is adequate in resisting applied loads given the parameters and assumption within this report. Design moments and axial forces along with positive and negative moment capacities are listed in Table 16.

Table 16. Design Moments/Forces and Moment Capacities

Design Section	Moment Demand (kip-ft)	Axial Demand (kip)	Moment Capacity (kip-ft)
positive: interior deck	21.36	-	35.63
negative: interior deck	18.28	-	47.03
negative: overhang, design case I A-A	37.22	10.52	47.03
negative: overhang, design case I B-B	36.88	9.99	47.03
negative: overhang, design case I C-C	32.05	9.54	47.03
negative: overhang, design case III D-D	5.63	-	47.03
negative: overhang, design case III E-E	6.70	-	47.03

The maximum positive design moment in the interior region of the deck is 21.36 kip-ft while the positive moment capacity of the cross section is 35.63 kip-ft. The maximum negative design moment is found to occur in the overhang region and is 37.22 kip-ft with an accompanied 10.52 kip axial tension force. The cross section is capable of resisting a 47.03 kip-ft moment with no axial load. A negative moment of 37 kip-ft can be accompanied with an approximate axial load of 35 kip and be within the interaction curve limits for this cross section. Thus the T-beam is adequate in resisting the load demands of the overhang region.

When compared to the traditional reinforced concrete deck examples presented in Chapter 1, the UHPC positive moment capacity is approximately 20% higher. Positive moment capacities for the concrete girder and steel plate girder superstructure examples are 30.79 kip-ft and 29.52 kip-ft, respectfully. The negative moment capacity of the UHPC deck is within the capacity range for the overhang of the two examples. Negative overhang moment capacities for the presented concrete girder and steel plate girder superstructure examples are 43.02 kip-ft and 65.40 kip-ft. The negative moment capacity of the UHPC cross section is 47.03 kip-ft. A direct comparison of the negative moment capacity for the overhang region between the example decks and the UHPC is not straightforward. The collision capacity of the railing greatly influences the moment which must be resisted during the design of the deck. The best comparison available is between the reinforced concrete deck supported on the concrete girder superstructure and the UHPC cross section of this report since the same concrete parapet is used for both. The negative moment capacity of the UHPC is approximately 10% higher when compared to the traditional reinforced concrete deck.

An oversized UHPC section may be desirable until more confidence is gained in the behavior and design of UHPC decks. This example does illustrate that a UHPC deck panel is capable to resist loads due to traffic and collision, but should be further verified through experimental studies on UHPC decks to support assumptions and flexural methodology made through this analysis. With additional data, the flexural behavior methodology of UHPC deck panel can be further established and more efficient use of UHPC can be realized.

REFERENCES

1. Graybeal, B.A., "Material Property Characterization of Ultra-High Performance Concrete," Federal Highway Administration, Report No. FHWA-HRT-06-103, August 2006, 186 pp.
2. Graybeal, B.A., "Structural Behavior of Ultra-High Performance Concrete Prestressed I-Girders," Federal Highway Administration, Report No. FHWA-HRT-06-115, August 2006, 104 pp.
3. Toutlemonde, F., J. Resplendino, L. Sorelli, S. Bouteille, and S. Brisard, "Innovative Design of Ultra High-Performance Fiber Reinforced Concrete Ribbed Slab: Experimental Validation and Preliminary Detailed Analyses," In. H.G. Russel, Ed., *Seventh International Symposium on Utilization of High-Strength/High-Performance Concrete*, SP-228, 2005, pp. 1187-1206, Detroit, MI: American Concrete Institute.
4. Wassef, W.G., et al., "Comprehensive Design Example for Prestressed Concrete (PSC) Girder Superstructure Bridge with Commentary (in US Customary Units)," Modjeski and Masters, Inc., Report No. FHWA-NHI-04-043, November 2003, 381 pp.
5. Hartle, R.A., et al., "LRFD Design Example for Steel Girder Superstructure Bridge with Commentary," Michael Baker Jr., Inc., Report No. FHWA NHI-04-041, December 2003, 644 pp.
6. AASHTO, *AASHTO LRFD Bridge Design Specifications, 3rd Edition*, American Association of State Highway and Transportation Officials, 2006.
7. Caltrans, "Seismic Design Criteria", California Department of Transportation, June 2006.
8. Graybeal, B.A., "Compressive Behavior of an Ultra-High Performance Fiber Reinforced Concrete," *ACI Materials Journal*, V. 104, No. 2, Mar.-Apr. 2007, pp. 146-152.

DISCLAIMER

- ❖ This document has been reproduced from the best copy furnished by the sponsoring agency.